

SHARPER ANALYSIS OF SINGLE-LOOP METHODS FOR BILEVEL OPTIMIZATION

005 **Anonymous authors**

006 Paper under double-blind review

ABSTRACT

011 Bilevel optimization underpins many machine learning applications, including
 012 hyperparameter optimization, meta-learning, neural architecture search, and re-
 013inforcement learning. While hypergradient-based methods have advanced sig-
 014nificantly, a gap persists between theoretical guarantees—typically derived for
 015 multi-loop algorithms—and practical single-loop implementations required for ef-
 016ficiency. This work narrows that gap by establishing sharper convergence results
 017 for single-loop approximate implicit differentiation (AID) and iterative differenti-
 018ation (ITD) methods. For AID, we improve the convergence rate from $\mathcal{O}(\kappa^6/K)$
 019 to $\mathcal{O}(\kappa^5/K)$, where κ is the condition number of the inner-level problem. For
 020 ITD, we prove that the asymptotic error is $\mathcal{O}(\kappa^2)$, exactly matching the known
 021 lower bound and improving upon the previous $\mathcal{O}(\kappa^3)$ guarantee. We further val-
 022 idate the refined analyses by the experiments on synthetic bilevel optimization
 023 tasks.

1 INTRODUCTION

027 Bilevel optimization has attracted extensive attention in various applications of machine learning,
 028 including hyperparameter optimization (Maclaurin et al., 2015; Franceschi et al., 2017; Shaban et al.,
 029 2019; Shen et al., 2024), meta-learning (Chen et al., 2017; Finn et al., 2017; Franceschi et al., 2018),
 030 neural architecture search (Liu et al., 2018; He et al., 2020), and reinforcement learning (Zhang
 031 et al., 2020; Wang et al., 2020; Shen et al., 2025). Bilevel optimization corresponds to solving one
 032 optimization problem subject to constraints defined by another optimization problem. In this paper,
 033 we focus on the following bilevel optimization problem:

$$\min_{x \in \mathbb{R}^m} \Phi(x) = f(x, y^*(x)) \quad \text{s.t.} \quad y^*(x) = \arg \min_{y \in \mathbb{R}^n} g(x, y), \quad (1)$$

036 where the outer- and inner-level functions f and g are both jointly continuously differentiable on
 037 $\mathbb{R}^m \times \mathbb{R}^n$. We focus on the setting where g is strongly convex with respect to (w.r.t.) the inner-level
 038 variable y , which can guarantee the uniqueness of the inner solution (Chen et al., 2024).

039 Hypergradient-based algorithms have recently gained significant attention for their balance of sim-
 040 plicity and efficiency. Two prominent approaches are approximate implicit differentiation (AID)
 041 (Domke, 2012; Pedregosa, 2016; Ghadimi & Wang, 2018; Grazzi et al., 2020; Ji et al., 2021) and it-
 042 erative differentiation (ITD) (Franceschi et al., 2017; Shaban et al., 2019; Grazzi et al., 2020; Ji et al.,
 043 2021; Liu et al., 2021). The key distinction lies in how they estimate the hypergradient $\nabla \Phi(x)$: AID
 044 leverages the implicit function theorem, while ITD applies automatic differentiation (see Section 2).
 045 Despite this difference, both methods require solving the inner problem to obtain the optimal solu-
 046 tion y^* . In practice, however, closed-form solutions are rarely available, and one typically resorts to
 047 gradient descent to compute an approximate solution \hat{y} .

048 Most theoretical studies of bilevel optimization analyze algorithms that employ **multi-loop** updates
 049 (multi-step gradient descent) for the inner problem and linear-system (Ghadimi & Wang, 2018; Ji
 050 et al., 2021; Dong et al., 2025; Fang et al., 2025). In contrast, practical algorithms overwhelmingly
 051 adopt **single-loop** updates, where only one inner update is performed per outer iteration. The main
 052 appeal of single-loop methods is computational efficiency: they significantly reduce training cost
 053 while maintaining competitive performance. This design has become standard across a wide range
 of applications. For instance, in neural architecture search, DARTS (Liu et al., 2018) updates the

Algorithms	Convergence rate	$MV(\epsilon)$	$Gc(\epsilon)$
AID (Ji et al., 2022)	$\mathcal{O}(\kappa^6/K)$	$\mathcal{O}(\kappa^6\epsilon^{-1})$	$\mathcal{O}(\kappa^6\epsilon^{-1})$
AID (this paper)	$\mathcal{O}(\kappa^5/K)$	$\mathcal{O}(\kappa^5\epsilon^{-1})$	$\mathcal{O}(\kappa^5\epsilon^{-1})$
ITD (Ji et al., 2022)	$\mathcal{O}(\kappa^3/K + \kappa^3)$	N/A	N/A
ITD (this paper)	$\mathcal{O}(\kappa^3/K + \kappa^2)$	N/A	N/A
Lower bound of ITD	$\Omega(\kappa^2)$	N/A	N/A

Table 1: Comparison of computational complexities of both single-loop AID-based and ITD-based algorithms for finding an ϵ -stationary point. For the last three columns, ‘N/A’ means that the complexities to achieve an ϵ -accuracy are not measurable due to the nonvanishing convergence error. $MV(\epsilon)$: the total number of Jacobian- and Hessian-vector product computations. $Gc(\epsilon)$: the total number of gradient computations.

network parameters (y) via single-loop while optimizing architecture coefficients (x). In few-shot meta-learning, MAML (Finn et al., 2017) applies single-loop adaptation to task-specific parameters. In data reweighting for imbalanced or noisy samples, methods such as Ren et al. (2018); Shu et al. (2019) also rely on single-loop updates. These examples underscore a critical gap: while existing theory primarily addresses multi-loop schemes, the algorithms most relevant in practice depend on single-loop updates, making it essential to establish their convergence guarantees.

Recently, Liu et al. (2024) propose MEHA, a Moreau-envelope-based single-loop method with convergence rate $O(1/K^{1/2-p} + 1/K^p)$, where K is the number of outer iterations and $p \in (0, 1/2)$. Kwon et al. (2023b) design F³SA by incorporating momentum, achieving a rate of $O(K^{-2/3})$. However, these single-loop methods remain slower than AID and ITD, both of which can reach $O(K^{-1})$ as shown in Table 1. Motivated by this gap, we focus on the AID and ITD methods and seek sharper analyses for their single-loop variants.

Along similar lines, Ji et al. (2022) analyze different loop structures in bilevel optimization and establish corresponding theoretical results. For AID, Ji et al. (2022) establish a convergence of $\mathcal{O}(\kappa^6/K)$ in the single-loop setting, where $\kappa = \frac{L}{\mu}$ denotes the condition number (L and μ are the gradient Lipschitz and strong convexity constants defined respectively in Assumptions 1 and 3). This is still inferior to the $\mathcal{O}(\kappa^4/K)$ rate achieved by the multi-loop AID. Therefore, our work first aims to narrow the gap of the convergence between the single-loop and multi-loop AID-based methods:

- Our first contribution is that, via a refined analysis and a novel analytical methodology, we show that the single-loop AID algorithm can achieve a convergence rate of $\mathcal{O}(\kappa^5/K)$, thereby providing a more practical and theoretically grounded alternative for large-scale bilevel optimization tasks where previous guarantees of $\mathcal{O}(\kappa^6/K)$ limited reliability.

For ITD, Ji et al. (2022) show that single-loop suffers from an inherent error of order $\mathcal{O}(\kappa^3)$, leaving a gap of $\alpha\mu$ (with α the inner-level step size) from the fundamental lower bound. They identify closing this gap as an open problem.

- Our second contribution is that the single-loop ITD method can attain a convergence error of order $\mathcal{O}(\kappa^2)$, exactly matching the lower bound of Ji et al. (2022), thereby establishing its theoretical optimality and potentially supporting it as an efficient alternative to more costly multi-loop methods.

Moreover, our key technical contribution is a novel analytical framework that departs from the standard proof template. Prior analyses bound the squared error norm directly, which inflates the dependence on κ . We instead decouple the analysis by first bounding the error norm and only then squaring it. This delicate treatment avoids the overestimation and yields sharper bounds, providing a more accurate characterization of both AID and ITD.

2 ALGORITHMS

In this section, we introduce two popular bilevel optimization algorithms to solve problem (1). It is worth noting that we provide the single-loop algorithms, as this aligns with practical choices in related applications.

108

Algorithm 1 Single-Loop AID-based bilevel optimization algorithm

1: **Input:** Learning rates $\alpha, \beta, \eta > 0$, initializations x_0, y_0, v_0 .
2: **for** $k = 0, 1, 2, \dots, K$ **do**
3: Set $y_k^0 = \hat{y}_{k-1}$ if $k > 0$ and y_0 otherwise (**warm start initialization**)
4: Update $\hat{y}_k = y_k^0 - \alpha \nabla_y g(x_k, y_k^0)$
5: Set $v_k^0 = \hat{v}_{k-1}$ if $k > 0$ and v_0 otherwise (**warm start initialization**)
6: Update $\hat{v}_k = (I - \eta \nabla_y^2 g(x_k, \hat{y}_k))v_k^0 + \eta \nabla_y f(x_k, \hat{y}_k)$
7: Compute $\hat{\nabla} \Phi(x_k) = \nabla_x f(x_k, \hat{y}_k) - \nabla_{xy}^2 g(x_k, \hat{y}_k) \hat{v}_k$
8: Update $x_{k+1} = x_k - \beta \hat{\nabla} \Phi(x_k)$
9: **end for**

119

Algorithm 2 Single-Loop ITD-based bilevel optimization algorithm

1: **Input:** Learning rate $\alpha, \beta > 0$, initializations x_0 and y_0 .
2: **for** $k = 0, 1, 2, \dots, K$ **do**
3: Set $y_k^0 = \hat{y}_{k-1}$ if $k > 0$ and y_0 otherwise (**warm start initialization**)
4: Update $\hat{y}_k(x_k) = y_k^0 - \alpha \nabla_y g(x_k, y_k^0)$
5: Compute $\hat{\nabla} \Phi(x_k) = \nabla_x f(x_k, \hat{y}_k) - \alpha \nabla_{xy}^2 g(x_k, y_k^0) \nabla_y f(x_k, \hat{y}_k)$
6: Update $x_{k+1} = x_k - \beta \hat{\nabla} \Phi(x_k)$
7: **end for**

128

129

2.1 AID-BASED BILEVEL OPTIMIZATION ALGORITHM

131

We provide the single-loop AID-based bilevel optimization algorithm (for simplicity, hereafter referred to as AID) in Algorithm 1. In each outer-level iteration k , AID first performs one step of gradient descent on the inner-level function $g(x, y)$ to find a point \hat{y}_k that approximates y_k^* , where y_k^* denotes $\arg \min_y g(x_k, y)$. Moreover, to accelerate the practical training process, AID usually adopts a warm-start strategy. In other words, the initial value y_k^0 of the inner-level problem at iteration k is set to the updated value \hat{y}_{k-1} from iteration $k - 1$.

138

In the outer-level, AID first obtain \hat{v}_k via solving a linear system $\nabla_y^2 g(x_k, \hat{y}_k)v = \nabla_y f(x_k, \hat{y}_k)$ by one step of gradient descent starting from v_k^0 , and then AID can estimate the gradient $\nabla \Phi(x_k) = \nabla_x f(x_k, y_k^*) - \nabla_{xy}^2 g(x_k, y_k^*) \hat{v}_k$ of the outer-level function w.r.t. x (called hypergradient) by the form of $\hat{\nabla} \Phi(x_k) = \nabla_x f(x_k, \hat{y}_k) - \nabla_{xy}^2 g(x_k, \hat{y}_k) \hat{v}_k$.

143

144

2.2 ITD-BASED BILEVEL OPTIMIZATION ALGORITHM

145

We present the single-loop ITD-based bilevel optimization algorithm (for simplicity, hereafter referred to as ITD) in Algorithm 2. Similar to AID, ITD also performs one step of gradient descent and employs a warm-start strategy on the inner-level function $g(x, y)$ to obtain \hat{y}_k . Unlike AID, however, ITD does not rely on the implicit gradient formula when estimating the hypergradient, but instead estimates the hypergradient directly via automatic differentiation. Since the update of \hat{y}_k depends on x_k , ITD needs to store the iterative trajectory for backpropagation. In this work, because we consider the more practical single-step gradient descent, the hypergradient estimate takes the following form: $\hat{\nabla} \Phi(x_k) = \nabla_x f(x_k, \hat{y}_k) - \alpha \nabla_{xy}^2 g(x_k, y_k^0) \nabla_y f(x_k, \hat{y}_k)$.

154

155

3 DEFINITIONS AND ASSUMPTIONS

156

157

In bilevel optimization, the objective is to minimize the hyper-objective function $\nabla \Phi(x)$, which is typically nonconvex. Because finding a global minimum for such functions can be computationally prohibitive (Nemirovski & IUDin, 1983), this work aims to find an approximate stationary point following the literature (Carmon et al., 2017; Ji et al., 2021).

161

Definition 1. We call \bar{x} is an ϵ -stationary point of problem (1) if $\|\nabla \Phi(\bar{x})\|^2 \leq \epsilon$.

162 In this work, we focus on the problem (1) under the following standard assumptions, as also widely
 163 adopted by Ghadimi & Wang (2018); Ji et al. (2021). Let $z = (x, y)$ denote all parameters.
 164

165 **Assumption 1.** *The inner-level function $g(x, y)$ is μ -strong-convex w.r.t. y .*

166 **Assumption 2.** *The function $f(z)$ is M -Lipschitz, i.e., for any z, z' ,*

$$167 \quad |f(z) - f(z')| \leq M \|z - z'\|. \\ 168$$

169 **Assumption 3.** *Gradients $\nabla f(z)$ and $\nabla g(z)$ are L -Lipschitz, i.e., for any z, z' ,*

$$170 \quad \|\nabla f(z) - \nabla f(z')\| \leq L \|z - z'\|, \quad \|\nabla g(z) - \nabla g(z')\| \leq L \|z - z'\|. \\ 171$$

172 **Assumption 4.** *Suppose the derivatives $\nabla_{xy}^2 g(z)$ and $\nabla_y^2 g(z)$ are ρ -Lipschitz, i.e., for any z, z' ,*

$$173 \quad \|\nabla_{xy}^2 g(z) - \nabla_{xy}^2 g(z')\| \leq \rho \|z - z'\|, \quad \|\nabla_y^2 g(z) - \nabla_y^2 g(z')\| \leq \rho \|z - z'\|. \\ 174$$

175 4 MAIN RESULTS

176 In this section, we will provide the convergence analysis and characterize the overall computational
 177 complexity for both single-loop AID- and ITD-based algorithms.

180 4.1 CHALLENGES IN THE ANALYSIS AND OUR APPROACH

182 The conventional analytical path (Ji et al., 2021; 2022), which we term *Direct Squared Norm Analysis* (DSNA),
 183 relies on bounding the squared norm of the error vector at each iteration. Let's consider a simplified one-step error recurrence of the form $e_{k+1} = Ae_k + \delta_k$, where A represents the
 184 contraction operator and δ_k is the accumulated error term (e.g., from the inexact inner-loop solution). The standard approach proceeds by analyzing its squared norm: $\|e_{k+1}\|^2 = \|Ae_k + \delta_k\|^2 =$
 185 $\|Ae_k\|^2 + 2\langle Ae_k, \delta_k \rangle + \|\delta_k\|^2$. The primary challenge arises from the cross-term, $2\langle Ae_k, \delta_k \rangle$. To
 186 make this term tractable, existing analyses invariably resort to “pessimistic” inequalities, such as
 187 the Cauchy-Schwarz or Young’s inequality (e.g., $2\langle a, b \rangle \leq \|a\|^2 + \|b\|^2$). For example, Ji et al.
 188 (2022) adopted this approach when analyzing the error upper bounds of the inner variable and the
 189 solution of the linear system. While this decouples the terms, it does so at a great cost. This step
 190 fundamentally ignores any potential underlying structure or cancellation effects between e_k and δ_k .
 191 The repeated application of such loose bounds over many iterations causes the dependencies on the
 192 problem’s condition number, κ , to compound, ultimately leading to the inflated convergence rate.
 193 Our key insight is that this pessimistic rate is not an inherent property of the algorithm itself, but
 194 rather an analysis artifact stemming from the premature squaring of the norm. This step discards
 195 crucial information too early in the derivation.

196 We introduce a more delicate analytical strategy, *Decoupled Norm Analysis* (DNA), that sidesteps
 197 this bottleneck. Instead of immediately squaring the error recurrence, we first analyze the error norm
 198 in its linear form by applying the triangle inequality: $\|e_{k+1}\| = \|Ae_k + \delta_k\| \leq \|Ae_k\| + \|\delta_k\|$. By
 199 keeping the analysis in the linear domain of norms for as long as possible, we can establish a tighter
 200 recursive relationship (Lemmas 1 and 2 for AID, Lemma 5 for ITD). This approach allows for a
 201 more refined handling of the error terms, preserving more of the underlying geometric structure.
 202 The squaring operation is deferred to the very end of the analysis, after the full recurrence has been
 203 unrolled (Lemma 4 for AID, Lemma 7 for ITD). This seemingly simple change of order—analyzing
 204 the norm before squaring it—prevents the compounding of pessimistic estimates associated with the
 205 cross-term. It is this principled deviation from the standard analytical template that allows us to
 206 break the rate barrier and establish the significantly improved convergence rate, providing a more
 207 faithful theoretical picture of the algorithm’s efficiency.

210 4.2 CONVERGENCE ANALYSIS OF AID

212 **Proof Sketch:** The proof for AID consists of three main steps: 1) Decomposing the hypergradient
 213 estimation error into the approximation error of the inner-level solution and the error from solving
 214 the linear system. (Lemma 3). 2) Bounding these two types of errors based on the errors in previ-
 215 ous iterations (Lemmas 1 and 2). 3) Combining the results from the preceding steps to provide a
 convergence guarantee for the AID algorithm (Theorem 1).

Before presenting the convergence analysis on AID, we first give the following useful lemmas. Now we study the convergence of $\|\hat{v}_k - v_k^*\|$ and $\|\hat{y}_k - y_k^*\|$ for $k = 1, 2, \dots, K$, where v_k^* is the exact solution of the linear system $\nabla_y^2 g(x_k, \hat{y}_k)v = \nabla_y f(x_k, \hat{y}_k)$. Note that the descent of the overall outer-level objectives also depends on the error of y_k . We next analyze these errors.

Lemma 1. Consider single-loop AID-based algorithm in Algorithm 1. Suppose Assumptions 1-4 hold. Let $\alpha \leq \frac{1}{L}$, then we have

$$\|y_k^0 - \hat{y}_k\| \leq \alpha L (\|\hat{y}_{k-1} - y_{k-1}^*\| + \|x_{k-1} - x_k\|), \quad (2)$$

$$\|\hat{y}_k - y_k^*\| \leq (1 - \mu\alpha) \|\hat{y}_{k-1} - y_{k-1}^*\| + \frac{L}{\mu} \|x_{k-1} - x_k\|. \quad (3)$$

Remark 1. Lemma 1 demonstrates that: 1) for $k = 1, \dots, K$, the error between the initial point and the iterated solution of the inner-level problem in single-loop AID can be bounded by the error from the previous iteration; 2) the error between the approximate solution and the exact solution of the inner-level problem in single-loop AID can also be bounded by the error from the previous iteration, which serves as a crucial foundation for the analysis of the algorithm's convergence.

Then, we decompose $\|\hat{v}_k - v_k^*\|$ and then estimate the upper bound.

Lemma 2. Consider single-loop AID-based algorithm in Algorithm 1. Suppose Assumptions 1-4 hold. Let $C_0 = \frac{\rho M}{\mu^2} + \frac{L}{\mu}$. Then, we have

$$\|\hat{v}_k - v_k^*\| \leq \|\hat{v}_k - \tilde{v}_k^*\| + C_0 \|\hat{y}_k - y_k^*\|, \quad (4)$$

$$\|\hat{v}_k - \tilde{v}_k^*\| \leq (1 - \mu\eta) \|\hat{v}_{k-1} - \tilde{v}_{k-1}^*\| + C_0 (\|y_k^0 - \hat{y}_k\| + \|x_{k-1} - x_k\|), \quad (5)$$

where $\tilde{v}_k^* = (\nabla_y^2 g(x_k, \hat{y}_k))^{-1} \nabla_y f(x_k, \hat{y}_k)$.

Remark 2. The purpose of Lemma 2 is to conduct a more detailed decomposition of the error between \hat{v}_k and v_k^* , because this error originates from two aspects: 1) The use of \hat{y}_k to approximate y_k^* in the inner-level problem. 2) The use of \hat{v}_k , obtained from solving the linear system $\nabla_y^2 g(x_k, \hat{y}_k)v = \nabla_y f(x_k, \hat{y}_k)$, to approximate v_k^* . Therefore, Lemma 2 decouples these two factors and controls them separately. Specifically, the first and second terms in Eq. (4) are only related to the precision of the linear equation solution and the inner-level problem solution, respectively. 3) Eq. (5) further expands the first term on the right-hand side of Eq. (4).

In Lemmas 1 and 2, we have already provided the relevant error terms of y_k and v_k . Therefore, we will utilize the above results to analyze the error between the estimated hypergradient $\hat{\nabla}\Phi(x_k)$ and the true hypergradient $\nabla\Phi(x_k)$.

Lemma 3. Consider single-loop AID-based algorithm in Algorithm 1. Suppose Assumptions 1-4 hold. Define C_0 as in Lemma 2. Then we have

$$\|\hat{\nabla}\Phi(x_k) - \nabla\Phi(x_k)\| \leq \left(L + \frac{\rho M}{\mu} + C_0 L \right) \|\hat{y}_k - y_k^*\| + L \|\hat{v}_k - \tilde{v}_k^*\|. \quad (6)$$

Unlike the previous DSNA, our proposed DNA avoids the inflation of the condition number κ caused by repeated squaring. Combine Eq. (6) with the former lemmas, we can get the following lemma.

Lemma 4. Consider single-loop AID-based algorithm in Algorithm 1. Suppose Assumptions 1-4 hold. Define C_0 as in Lemma 2. Let $\alpha = \eta = \frac{1}{L}$, $C_1 = \frac{4C_0L}{\mu}$, $C_2 = \frac{\alpha L^2 C_0}{\mu} + \frac{\rho M}{\mu^2} + \frac{L}{\mu} + \frac{LC_1}{\mu}$ and $C_3 = L + \frac{\rho M}{\mu} + C_0 L$. Choose the outer stepsize β such that $\beta = \min\{\frac{C_1\mu\alpha}{4C_2C_3}, \frac{\eta\mu}{2LC_2}\}$. Then, we have

$$\begin{aligned} \|\hat{\nabla}\Phi(x_k) - \nabla\Phi(x_k)\|^2 &\leq L^2 \left(1 - \frac{\mu}{4L}\right)^k \cdot \left(\|v_0^Q - \tilde{v}_0^*\| + C_1 \|y_0^N - y_0^*\|\right)^2 \\ &\quad + \frac{3\beta^2 C_2^2 L^3}{\mu} \sum_{t=0}^k \left(1 - \frac{\mu}{4L}\right)^{k-1-t} \|\nabla\Phi(x_t)\|^2. \end{aligned} \quad (7)$$

Remark 3. Lemma 4 is a key result that supports the convergence analysis of single-loop AID-based algorithm. Compared to the work of (Ji et al., 2022), we relax the limit of the step-size for solving the linear system. Specifically, Ji et al. (2022) in their Corollary 2 required that $\eta = \mathcal{O}(\kappa^{-2})$, whereas we, through a more fine-grained analysis, set eta to $1/L$. This indirectly allows for a more aggressive choice of the outer-level step size β , thereby achieving a faster convergence rate.

270 Based on the above conclusions, the following theorem provides a convergence analysis for single-
 271 loop AID-based algorithm.

273 **Theorem 1.** Consider single-loop AID-based algorithm in Algorithm 1. Suppose Assumptions
 274 1-4 hold. Choose parameters $\alpha = \eta = \frac{1}{L}$. Let $L_\Phi = L + \frac{2L^2 + \rho M^2}{\mu^2} + \frac{2\rho LM + L^3}{\mu^2} +$
 275 $\frac{\rho L^2 M}{\mu^3}$ be the smoothness parameter of $\Phi(\cdot)$ ^a. Choose the outer stepsize β such that
 276 $\beta = \min\{\frac{C_1 \mu \alpha}{4C_2 C_3}, \frac{\eta \mu}{2LC_2}\}$. Then, $\frac{1}{K} \sum_{k=0}^{K-1} \|\nabla \Phi(x_k)\|^2 = \mathcal{O}(\frac{\kappa^5}{K})$, and the complexity is
 277 $Gc(\epsilon) = \tilde{\mathcal{O}}(\kappa^5 \epsilon^{-1})$, $Mv(\epsilon) = \tilde{\mathcal{O}}(\kappa^5 \epsilon^{-1})$.

278 ^aFor the origin of L_Φ , please refer to Lemma 8.

280 **Remark 4.** Compared with the work of Ji et al. (2022), our core improvement lies in controlling the
 281 errors of both the inner solution y and the linear system solution v , where we relax the requirement
 282 on the outer objective learning rate β from $\mathcal{O}(\kappa^{-6})$ to $\mathcal{O}(\kappa^{-5})$. Consequently, we improve the
 283 convergence rate of single-loop AID-based algorithm from $\mathcal{O}(\kappa^6/K)$ to $\mathcal{O}(\kappa^5/K)$. This indicates
 284 that the convergence gap between such algorithms and the AID algorithms with multi-step gradient
 285 descent is not as large as the $\mathcal{O}(\kappa^2)$ gap shown by Ji et al. (2022), but rather a smaller $\mathcal{O}(\kappa^1)$. This
 286 also partially supports the practice that most bilevel optimization algorithms perform only one or a
 287 few inner updates.

288 **Theorem 2. [Simplified version of the upper bound in Ji et al. (2022)].** Consider single-
 289 loop AID-based algorithm in Algorithm 1. Under the same setting of Theorem 1, we have
 290 $\frac{1}{K} \sum_{k=0}^{K-1} \|\nabla \Phi(x_k)\|^2 = \mathcal{O}(\frac{\kappa^6}{K})$.

293 4.3 CONVERGENCE ANALYSIS OF ITD

295 **Proof Sketch:** Unlike AID, the hypergradient estimation error of the single-loop ITD-based algo-
 296 rithm is introduced only by solving the inner problem. Therefore, our proof consists of three main
 297 steps: 1) Establishing the connection between the hypergradient estimation error and the approx-
 298 imation error of the inner-level solution (Lemma 6). 2) Bounding the approximation error of the
 299 solution to the inner-level problem (Lemma 5). 3) Combining the results from the previous steps to
 300 provide a convergence analysis for the ITD algorithm (Lemma 7 and Theorem 3).

301 To this end, we first present several useful lemmas, which will subsequently be used to prove Theo-
 302 rem 3.

303 **Lemma 5.** Consider the single-loop ITD-based algorithm in Algorithm 2. Suppose Assumptions
 304 1-4 hold. Let $\alpha \leq \frac{1}{L}$, $C_4 = L + \alpha L^2 + \alpha \rho M$, $C_5 = M(1 - \alpha \mu) \frac{L}{\mu} + \alpha^2 \rho M^2$, $C_6 = 1 - \mu \alpha + \frac{L \beta C_4}{\mu}$
 305 and $C_7 = \frac{L \beta C_5}{\mu}$. Then, we have

$$307 \|\hat{y}_k - y^*(x_k)\| \leq C_6 \|\hat{y}_{k-1} - y^*(x_{k-1})\| + \frac{L\beta}{\mu} \|\nabla \Phi(x_{k-1})\| + C_7, \quad (8)$$

$$309 \|\hat{y}_k - y^*(x_k)\| \leq \left(1 - \frac{\mu}{2L}\right)^k \|\hat{y}_0 - y^*(x_0)\| + \frac{L\beta^2}{\mu} \sum_{j=0}^{k-1} \left(1 - \frac{\mu}{2L}\right)^{k-1-j} (\|\nabla \Phi(x_j)\| + C_5). \quad (9)$$

313 Using the error bound for $\|\hat{y}_k - y^*\|$, we will analyze the error between the estimated hypergradient
 314 $\hat{\nabla} \Phi(x_k)$ and the true hypergradient $\nabla \Phi(x_k)$ of the ITD algorithm in the following lemma.

316 **Lemma 6.** Consider the single-loop ITD-based algorithm in Algorithm 2. Suppose Assumptions
 317 1-4 hold. Define C_4 and C_5 in Lemma 5. Let $\alpha \leq \frac{1}{L}$, we have

$$318 \|\hat{\nabla} \Phi(x_k) - \nabla \Phi(x_k)\| \leq C_4 \|\hat{y}_k - y^*\| + C_5. \quad (10)$$

320 **Remark 5.** Lemma 6 shows that the error between the true hypergradient and the estimated hyper-
 321 gradient is controlled by the accuracy of the inner-level problem solution and an inherent error, part
 322 of which arises from $\|y_k^0 - \hat{y}_k\|$. This indicates that this non-vanishing convergence error is related
 323 to the refinement of the inner-level problem solution, and that the single-loop method is insufficient
 to bridge this gap.

324 **Lemma 7.** Consider the single-loop ITD-based algorithm in Algorithm 2. Suppose Assumptions
 325 1-4 hold. Define C_4 and C_5 in Lemma 5. Let $\alpha \leq \frac{1}{L}$ and $\beta \leq \frac{\mu^3}{2L(2L^2+\rho M)}$. Then we have
 326

$$327 \quad \left\| \widehat{\nabla} \Phi(x_k) - \nabla \Phi(x_k) \right\|^2 \leq C_4^2 \left(1 - \frac{\mu}{4L}\right)^k \|\hat{y}_0 - y^*(x_0)\|^2 \\ 328 \quad + \frac{3L\beta^2 C_4^2}{\mu} \sum_{j=0}^{k-1} \left(1 - \frac{\mu}{4L}\right)^{k-1-j} (\|\nabla \Phi(x_j)\| + C_5)^2 + 3C_5^2. \\ 329 \\ 330 \\ 331$$

332 Based on the above results, the following theorem provides a convergence analysis for single-loop
 333 ITD-based algorithm.
 334

335 **Theorem 3.** Consider the single-loop ITD-based algorithm in Algorithm 2. Suppose Assumptions
 336 1-4 hold. Choose parameters $\alpha = \eta = \frac{1}{L}$. Let $L_\Phi = L + \frac{2L^2+\rho M^2}{\mu^2} +$
 337 $\frac{2\rho LM+L^3}{\mu^2} + \frac{\rho L^2 M}{\mu^3}$ be the smoothness parameter of $\Phi(\cdot)$. Choose the outer stepsize β such
 338 that $\beta \leq \frac{\mu^3}{2L(2L^2+\rho M)}$. Then, $\frac{1}{K} \sum_{k=0}^{K-1} \|\nabla \Phi(x_k)\|^2 = \mathcal{O} \left(\frac{\kappa^3}{K} + \kappa^2 \right)$.
 339
 340
 341

342 **Remark 6.** Theorem 3 demonstrates that for the single-loop ITD-based algorithm, the convergence
 343 bound contains a non-vanishing error of order $\mathcal{O}(\kappa^2)$. Under the standard Assumptions 1-4, such
 344 an error is unavoidable. Moreover, this error upper bound of order $\mathcal{O}(\kappa^2)$ matches the error lower
 345 bound (Theorem 4), which indicates that we have achieved a tighter error upper bound through more
 346 refined analysis. This resolves the issue in Ji et al. (2022) where there exists a gap of $\alpha\mu$ between
 347 the upper and lower bounds.

348 **Theorem 4. [Simplified version of the lower bound in Ji et al. (2022)].** Consider the single-loop
 349 ITD-based algorithm in Algorithm 2. Suppose Assumptions 1-4 hold. Let $\alpha \leq \frac{1}{L}$, $\beta \leq \frac{1}{L_\Phi}$ and
 350 $L_\Phi = L + \frac{2L^2+\rho M^2}{\mu^2} + \frac{2\rho LM+L^3}{\mu^2} + \frac{\rho L^2 M}{\mu^3}$. Then, we have $\|\nabla \Phi(x_K)\|^2 \geq \Theta(\kappa^2)$.
 351

352 5 EXPERIMENTS

354 **Experimental setup.** We consider the following bilevel optimization problem:
 355

$$356 \quad f(x, y) = \frac{1}{2} x^T Z_x x + \frac{1}{10} \mathbf{1}^T y, \quad g(x, y) = \frac{1}{2} y^T Z_y y - Lx^T y + \mathbf{1}^T y, \\ 357$$

358 where $x, y \in \mathbb{R}^2$ and $Z_x = Z_y = \begin{bmatrix} L & 0 \\ 0 & \mu \end{bmatrix}$. Thus the optimal solution of the inner-level subproblem
 359 and the exact hypergradient have the following form:
 360

$$361 \quad y^*(x) = Z_y^{-1}(Lx - \mathbf{1}), \quad \nabla \Phi(x) = Z_x x + LZ_y^{-1} \mathbf{1}. \quad (11) \\ 362$$

363 Based on the updates of single-loop ITD-based method, we have $\hat{y}_k = y_k^0 - \alpha(Z_y y_k^0 - Lx_k + \mathbf{1})$.
 364 Let the hyperparameters set as $\mu = 0.1$, $M = 0.1$, $\rho = 0.1$, $K = 10000$ and $\alpha = 1/L$.

365 **Results of AID-based Algorithm.** Figure 1 presents the error curves of the single-loop AID-based
 366 Algorithm. In Figure 1 (Left), we compare the error upper bound derived by Thoerem 1 with that
 367 given by Ji et al. (2022) under different condition numbers κ . It can be observed that, under varying
 368 condition numbers, our upper bound curve consistently lies closer above the $\|\nabla \Phi(x_k)\|^2$ curve.
 369 This is achieved by refining the analysis and reducing the theoretical order of the upper bound from
 370 $\mathcal{O}(\kappa^6)$ to $\mathcal{O}(\kappa^5)$. In Figure 1 (Right), under the condition number $\kappa = 2$, we compare the variation
 371 of the error upper bound with respect to the number of outer iterations K . It can be seen that
 372 the $\|\nabla \Phi(x_k)\|^2$ curve keeps decreasing as the number of iterations increases, which indicates that
 373 the single-loop AID-based algorithm converges as K grows, thereby confirming the correctness of
 374 Theorem 1. Moreover, we observe that our upper bound curve consistently outperforms that of Ji
 375 et al. (2022), which demonstrates that, theoretically, we provide a tighter error upper bound for this
 376 algorithm, thus verifying the correctness and effectiveness of our theoretical results.
 377

Results of ITD-based Algorithm. Figure 2 illustrates the performance of the ITD-based algorithm.
 378 From Figure 2 (Left), we first observe that in Ji et al. (2022), the gap between the reported upper and

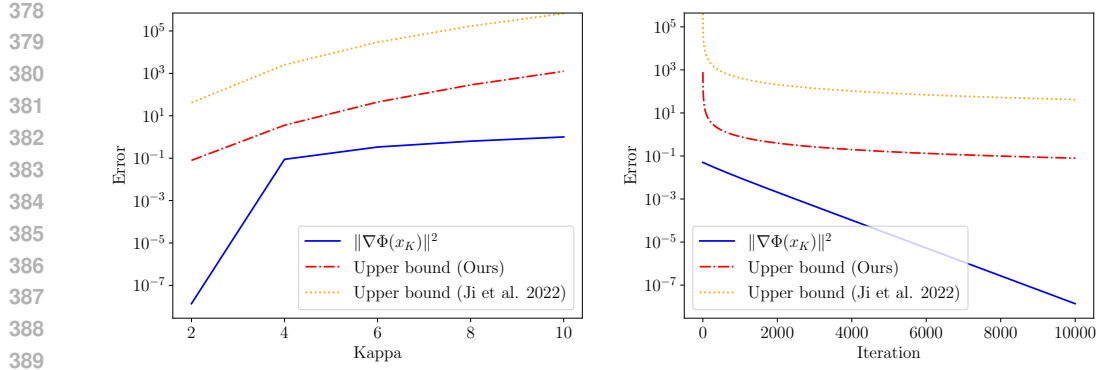


Figure 1: Comparison of error curves of the single-loop AID-based Algorithm. **Left:** Curves of various error terms (the squared norm of the true hypergradient $\|\nabla\Phi(x_K)\|^2$, the upper bound provided in Theorem 1 by us, and the upper bound provided in Theorem 2 by Ji et al. (2022)) with respect to different condition numbers κ . **Right:** Curves of various error terms with respect to the number of iterations K when the condition number $\kappa = 2$.

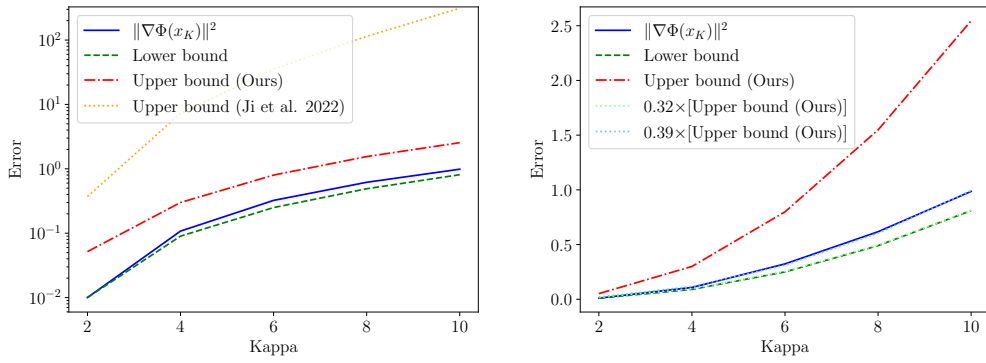


Figure 2: Comparison of error curves of the single-loop ITD-based Algorithm. **Left:** Curves of various error terms (the squared norm of the true hypergradient $\|\nabla\Phi(x_K)\|^2$, the upper bound provided in Theorem 3 by us, and the upper bound provided by Ji et al. (2022), the lower bound provided in Theorem 4) with respect to different condition numbers κ . **Right:** Curves of the scaled upper bound ($\times 0.32$ and $\times 0.39$) with respect to different condition numbers κ .

lower bounds remains large, confirming their conclusion that both bounds still differ by an error of order $\alpha\mu$. In contrast, our theoretical upper bound is substantially tighter: it lies much closer to the empirical $\|\nabla\Phi(x_K)\|^2$ curve while remaining strictly above it. This demonstrates that our bound provides a sharper characterization of the true convergence behavior.

To further verify the validity of our theoretical results, in addition to the curve of the true hypergradient norm, the upper bound curve (according to Theorem 3), and the lower bound curve, we also scale the upper bound curve in Figure 2 (Right). Specifically, we multiply it by 0.32 and 0.39, respectively. The results show that, after scaling the upper bound curve with different factors, its error values almost coincide with the true hypergradient norm curve and the lower bound curve, respectively. This indicates that the difference between the upper bound and the lower bound arises from constant factors introduced by scaling, rather than from differences in order. Thus, this supports the conclusion of Theorem 3, namely that we have reduced the inherent error to $\mathcal{O}(\kappa^2)$.

6 RELATED WORK

Hypergradient-based bilevel optimization. A variety of hypergradient-based bilevel algorithms have been proposed, differing mainly in how they estimate hypergradients. Methods based on approximate implicit differentiation (AID) (Domke, 2012; Pedregosa, 2016; Ghadimi & Wang, 2018;

Graffi et al., 2020; Ji et al., 2021) estimate the product of the inverse hessian and a vector by solving linear systems with efficient iterative solvers. In contrast, iterative differentiation (ITD) methods (Maclaurin et al., 2015; Franceschi et al., 2017; Shaban et al., 2019; Liu et al., 2021) compute hypergradients by backpropagating through the inner optimization trajectory. The convergence properties of AID- and ITD-based algorithms have been the subject of extensive study. For example, Ghadimi & Wang (2018) and Ji et al. (2021) analyzed the convergence rates and complexities of both approaches, while Ji et al. (2022) provided a unified framework covering different inner-loop choices and established lower bounds on the inherent error of ITD. Despite this progress, a notable gap remains between the convergence rate of the single-loop and multi-loop algorithms. Motivated by this gap, our work develops sharper convergence guarantees for single-loop methods, which are widely used in practice. Compared with Ji et al. (2022), our analysis for AID achieves an improved convergence order, while for ITD we refine the upper bound on the inherent error to match its known lower bound.

Gradient-based bilevel optimization. In recent years, some first-order gradient-based bilevel optimization methods have also attracted attention. Chen et al. (2025a) proposed an algorithm that achieves near-optimal complexity under the nonconvex-strongly convex setting; however, they still require a relatively large number of inner iterations, $O(\kappa \log(\lambda\kappa))$, where $\lambda = O(\kappa^3)$ denotes the penalty strength, which is also large. This, to some extent, affects practical applicability. In addition, Liu et al. (2024) proposed MEHA based on Moreau-envelope, where they considered the single-loop setting and provided a convergence rate of $O(1/K^{1/2-p} + 1/K^p)$, with $p \in (0, 1/2)$. Kwon et al. (2023b), by introducing momentum, designed F³SA, which is also a single-loop method and achieves a convergence rate of $O(K^{-2/3})$. However, compared with hypergradient-based methods, its convergence rate is relatively slower. Therefore, this paper focuses on providing a sharper analysis for hypergradient-based methods. From a technical perspective, DNA has the potential to be applied to such gradient-based methods (Chen et al., 2022; Hong et al., 2023; Liu et al., 2024; Fang et al., 2025), which we leave for future work.

The single-loop bilevel optimization algorithms. The single-loop methods have shown potential in many applications. In few-shot meta-learning, MAML (Finn et al., 2017), as a classic method, performs single-step gradient descent on the support set for multiple tasks in the inner-level, retaining the iteration path, while the outer-level updates the network’s initial values using the query set. In hyperparameter optimization, sample reweighting is a widely used application of bilevel optimization algorithms (Ren et al., 2018; Shu et al., 2019; Wang et al., 2024), as bilevel optimization can efficiently assign different weights to each sample. Such methods typically use the training set in the inner-level to perform single-step gradient descent to optimize model parameters, and the validation set in the outer loop to optimize sample weights or weighted networks. In neural architecture search, DARTS (Liu et al., 2018) method uses a one-step update in the inner-level to update the model, and the outer-level optimizes the architecture using validation data. It is worth noting that most of these algorithms achieve efficiency by single-loop, which is also crucial for the large-scale practice of bilevel optimization techniques (Choe et al., 2023; Shen et al., 2024). Therefore, in this work, we focus on the single-loop bilevel optimization algorithms, consistent with practical applications, and are committed to establishing sharper convergence guarantees for these algorithms.

7 CONCLUSION

In this work, we advance the theoretical understanding of single-loop bilevel optimization algorithms, a setting of growing practical relevance. For the AID method, our refined analysis improves the convergence rate to $\mathcal{O}(\kappa^5/K)$, narrowing the gap with multi-loop approaches. For the ITD method, we establish that its convergence error is exactly $\mathcal{O}(\kappa^2)$, thereby closing the open question raised in prior work regarding its tightness. Our experimental results can corroborate the theory, demonstrating that single-loop methods can achieve both efficiency and favorable convergence behavior. These findings not only bridge an important gap between theory and practice, but also potentially suggest that the single-loop bilevel optimization methods can be strong candidates for large-scale machine learning tasks. Beyond the specific result for the algorithm, we believe our proposed analytical paradigm of the decoupling norm analysis opens new path for studying other bilevel optimization algorithms, potentially tightening bounds for methods where previous analyses have been overly pessimistic.

486 **Limitations and Future Work.** We establish sharper convergence rates for single-loop bilevel
 487 methods under several technical assumptions. Among them, strong convexity and Hessian Lips-
 488 chitz may not always hold in deep neural networks, although these assumptions are standard in the
 489 bilevel optimization literature. Therefore, an important direction for future work is to relax these
 490 conditions and extend our analytical tools accordingly, and a promising direction is to replace the
 491 strong convexity assumption of the inner-level problem with the Polyak–Łojasiewicz (PL) condition
 492 (Polyak, 1967; Łojasiewicz, 1963), which have been validated in modern neural networks (Charles
 493 & Papailiopoulos, 2018; Liu et al., 2022b; Hardt & Ma, 2016; Liu et al., 2022a). In addition, we
 494 plan to further investigate various single-loop variants, including first-order methods and stochastic
 495 settings.

496 In future work, we plan to apply the proposed analytical technique to other bilevel optimization
 497 algorithms and settings, such as multi-loop structures (Ji et al., 2022), stochastic settings (Ji et al.,
 498 2021), and decentralized frameworks (Chen et al., 2025b). In addition, we will further investigate
 499 the robustness and scalability of these techniques, for example by extending them to other classes of
 500 optimization problems such as minimax optimization (Yang et al., 2024).

501 **Reproducibility Statement.** All results are theoretical, and complete proofs are provided in the
 502 appendix with clear assumptions and detailed derivations. This ensures that all claims can be inde-
 503 pendently verified without reliance on external data.

505 REFERENCES

507 Fan Bao, Guoqiang Wu, Chongxuan Li, Jun Zhu, and Bo Zhang. Stability and generalization of
 508 bilevel programming in hyperparameter optimization. *Advances in neural information processing
 509 systems*, 34:4529–4541, 2021.

510 Yair Carmon, John C Duchi, Oliver Hinder, and Aaron Sidford. Lower bounds for finding stationary
 511 points i. *arXiv preprint arXiv:1710.11606*, 2017.

512 Chih-Chung Chang and Chih-Jen Lin. LIBSVM: A library for support vector machines. *ACM
 513 Transactions on Intelligent Systems and Technology*, 2:27:1–27:27, 2011. Software available at
 514 <http://www.csie.ntu.edu.tw/~cjlin/libsvm>.

515 Zachary Charles and Dimitris Papailiopoulos. Stability and generalization of learning algorithms
 516 that converge to global optima. In *International conference on machine learning*, pp. 745–754.
 517 PMLR, 2018.

518 Lesi Chen, Jing Xu, and Jingzhao Zhang. On finding small hyper-gradients in bilevel optimization:
 519 Hardness results and improved analysis. In *The Thirty Seventh Annual Conference on Learning
 520 Theory*, pp. 947–980. PMLR, 2024.

521 Lesi Chen, Yaohua Ma, and Jingzhao Zhang. Near-optimal nonconvex-strongly-convex bilevel op-
 522 timization with fully first-order oracles. *Journal of Machine Learning Research*, 26(109):1–56,
 523 2025a.

524 Tianyi Chen, Yuejiao Sun, Quan Xiao, and Wotao Yin. A single-timescale method for stochastic
 525 bilevel optimization. In *International Conference on Artificial Intelligence and Statistics*, pp.
 526 2466–2488. PMLR, 2022.

527 Xuxing Chen, Minhui Huang, and Shiqian Ma. Decentralized bilevel optimization: X. chen et al.
 528 *Optimization Letters*, 19(7):1249–1313, 2025b.

529 Yutian Chen, Matthew W Hoffman, Sergio Gómez Colmenarejo, Misha Denil, Timothy P Lilli-
 530 crap, Matt Botvinick, and Nando Freitas. Learning to learn without gradient descent by gradient
 531 descent. In *International Conference on Machine Learning*, pp. 748–756. PMLR, 2017.

532 Sang Choe, Sanket Vaibhav Mehta, Hwileen Ahn, Willie Neiswanger, Pengtao Xie, Emma Strubell,
 533 and Eric Xing. Making scalable meta learning practical. *Advances in neural information process-
 534 ing systems*, 36:26271–26290, 2023.

535 Justin Domke. Generic methods for optimization-based modeling. In *Artificial Intelligence and
 536 Statistics*, pp. 318–326. PMLR, 2012.

540 Youran Dong, Junfeng Yang, Wei Yao, and Jin Zhang. Efficient curvature-aware hypergradient
 541 approximation for bilevel optimization. *arXiv preprint arXiv:2505.02101*, 2025.
 542

543 Sheng Fang, Yong-Jin Liu, Wei Yao, Chengming Yu, and Jin Zhang. qnbo: quasi-newton meets
 544 bilevel optimization. *arXiv preprint arXiv:2502.01076*, 2025.

545 Chelsea Finn, Pieter Abbeel, and Sergey Levine. Model-agnostic meta-learning for fast adaptation
 546 of deep networks. In *International conference on machine learning*, pp. 1126–1135. PMLR, 2017.

547

548 Luca Franceschi, Michele Donini, Paolo Frasconi, and Massimiliano Pontil. Forward and reverse
 549 gradient-based hyperparameter optimization. In *International conference on machine learning*,
 550 pp. 1165–1173. PMLR, 2017.

551

552 Luca Franceschi, Paolo Frasconi, Saverio Salzo, Riccardo Grazzi, and Massimiliano Pontil. Bilevel
 553 programming for hyperparameter optimization and meta-learning. In *International conference on*
 554 *machine learning*, pp. 1568–1577. PMLR, 2018.

555

556 Saeed Ghadimi and Mengdi Wang. Approximation methods for bilevel programming. *arXiv preprint*
 557 *arXiv:1802.02246*, 2018.

558

559 Riccardo Grazzi, Luca Franceschi, Massimiliano Pontil, and Saverio Salzo. On the iteration com-
 560 plexity of hypergradient computation. In *International Conference on Machine Learning*, pp.
 3748–3758. PMLR, 2020.

561

562 Moritz Hardt and Tengyu Ma. Identity matters in deep learning. *arXiv preprint arXiv:1611.04231*,
 563 2016.

564

565 Chaoyang He, Haishan Ye, Li Shen, and Tong Zhang. Milenas: Efficient neural architecture search
 566 via mixed-level reformulation. In *Proceedings of the IEEE/CVF Conference on Computer Vision*
 567 and *Pattern Recognition*, pp. 11993–12002, 2020.

568

569 Mingyi Hong, Hoi-To Wai, Zhaoran Wang, and Zhuoran Yang. A two-timescale stochastic algorithm
 570 framework for bilevel optimization: Complexity analysis and application to actor-critic. *SIAM*
Journal on Optimization, 33(1):147–180, 2023.

571

572 Kaiyi Ji, Junjie Yang, and Yingbin Liang. Bilevel optimization: Convergence analysis and enhanced
 573 design. In *International conference on machine learning*, pp. 4882–4892. PMLR, 2021.

574

575 Kaiyi Ji, Mingrui Liu, Yingbin Liang, and Lei Ying. Will bilevel optimizers benefit from loops.
 576 *Advances in Neural Information Processing Systems*, 35:3011–3023, 2022.

577

578 Jeongyeol Kwon, Dohyun Kwon, Stephen Wright, and Robert Nowak. On penalty methods
 579 for nonconvex bilevel optimization and first-order stochastic approximation. *arXiv preprint*
 580 *arXiv:2309.01753*, 2023a.

581

582 Jeongyeol Kwon, Dohyun Kwon, Stephen Wright, and Robert D Nowak. A fully first-order method
 583 for stochastic bilevel optimization. In *International Conference on Machine Learning*, pp. 18083–
 584 18113. PMLR, 2023b.

585

586 Yann LeCun, Léon Bottou, Yoshua Bengio, and Patrick Haffner. Gradient-based learning applied to
 587 document recognition. *Proceedings of the IEEE*, 86(11):2278–2324, 1998.

588

589 Bo Liu, Mao Ye, Stephen Wright, Peter Stone, and Qiang Liu. Bome! bilevel optimization made
 590 easy: A simple first-order approach. *Advances in neural information processing systems*, 35:
 591 17248–17262, 2022a.

592

593 Chaoyue Liu, Libin Zhu, and Mikhail Belkin. Loss landscapes and optimization in over-
 594 parameterized non-linear systems and neural networks. *Applied and Computational Harmonic*
 595 *Analysis*, 59:85–116, 2022b.

596

597 Hanxiao Liu, Karen Simonyan, and Yiming Yang. Darts: Differentiable architecture search. *arXiv*
 598 *preprint arXiv:1806.09055*, 2018.

594 Risheng Liu, Yaohua Liu, Shangzhi Zeng, and Jin Zhang. Towards gradient-based bilevel optimiza-
 595 tion with non-convex followers and beyond. *Advances in Neural Information Processing Systems*,
 596 34:8662–8675, 2021.

597 Risheng Liu, Zhu Liu, Wei Yao, Shangzhi Zeng, and Jin Zhang. Moreau envelope for nonconvex bi-
 598 level optimization: A single-loop and hessian-free solution strategy. In *International Conference*
 599 *on Machine Learning*, pp. 31566–31596. PMLR, 2024.

600 Stanislaw Łojasiewicz. Une propriété topologique des sous-ensembles analytiques réels. In *Les*
 601 *Équations aux Dérivées Partielles*, volume 117 of *Colloques Internationaux du CNRS*, pp. 87–
 602 89. Éditions du Centre National de la Recherche Scientifique, Paris, 1963.

603 Dougal Maclaurin, David Duvenaud, and Ryan Adams. Gradient-based hyperparameter optimiza-
 604 tion through reversible learning. In *International conference on machine learning*, pp. 2113–2122.
 605 PMLR, 2015.

606 A.S. Nemirovski and D.B. Iudin. *Problem Complexity and Method Efficiency in Optimization*. A
 607 Wiley-Interscience publication. Wiley, 1983. ISBN 9780471103455. URL <https://books.google.co.jp/books?id=6ULvAAAAMAAJ>.

608 Fabian Pedregosa. Hyperparameter optimization with approximate gradient. In *International con-
 609 ference on machine learning*, pp. 737–746. PMLR, 2016.

610 B. T. Polyak. A general method for solving extremal problems. *Doklady Akademii Nauk SSSR*, 174
 611 (1):33–36, 1967.

612 Mengye Ren, Wenyuan Zeng, Bin Yang, and Raquel Urtasun. Learning to reweight examples for
 613 robust deep learning. In *International conference on machine learning*, pp. 4334–4343. PMLR,
 614 2018.

615 Amirreza Shaban, Ching-An Cheng, Nathan Hatch, and Byron Boots. Truncated back-propagation
 616 for bilevel optimization. In *The 22nd international conference on artificial intelligence and statis-
 617 tics*, pp. 1723–1732. PMLR, 2019.

618 Han Shen and Tianyi Chen. On penalty-based bilevel gradient descent method. In *International
 619 conference on machine learning*, pp. 30992–31015. PMLR, 2023.

620 Han Shen, Pin-Yu Chen, Payel Das, and Tianyi Chen. Seal: Safety-enhanced aligned llm fine-tuning
 621 via bilevel data selection. *arXiv preprint arXiv:2410.07471*, 2024.

622 Han Shen, Zhuoran Yang, and Tianyi Chen. Principled penalty-based methods for bilevel reinforce-
 623 ment learning and rlhf. *Journal of Machine Learning Research*, 26(114):1–49, 2025.

624 Jun Shu, Qi Xie, Lixuan Yi, Qian Zhao, Sanping Zhou, Zongben Xu, and Deyu Meng. Meta-
 625 weight-net: Learning an explicit mapping for sample weighting. *Advances in neural information
 626 processing systems*, 32, 2019.

627 Lingxiao Wang, Qi Cai, Zhuoran Yang, and Zhaoran Wang. On the global optimality of model-
 628 agnostic meta-learning. In *International conference on machine learning*, pp. 9837–9846. PMLR,
 629 2020.

630 Quanziang Wang, Renzhen Wang, Yuexiang Li, Dong Wei, Hong Wang, Kai Ma, Yefeng Zheng,
 631 and Deyu Meng. Relational experience replay: Continual learning by adaptively tuning task-wise
 632 relationship. *IEEE Transactions on Multimedia*, 26:9683–9698, 2024.

633 Yifan Yang, Zhaofeng Si, Siwei Lyu, and Kaiyi Ji. First-order minimax bilevel optimization. *Ad-
 634 vances in Neural Information Processing Systems*, 37:24990–25035, 2024.

635 Haifeng Zhang, Weizhe Chen, Zeren Huang, Minne Li, Yaodong Yang, Weinan Zhang, and Jun
 636 Wang. Bi-level actor-critic for multi-agent coordination. In *Proceedings of the AAAI conference
 637 on artificial intelligence*, volume 34, pp. 7325–7332, 2020.

638

648 **A PROOF OF THE SINGLE-LOOP AID-BASED ALGORITHM**
 649

650 Firstly, we give the following useful lemma. Recall that $\Phi(x) = f(x, y^*(x))$ in Eq. (1). Then, we
 651 use the following lemma to characterize the Lipschitz properties of $\nabla\Phi(x)$, which is adapted from
 652 Lemma 2.2 in Ghadimi & Wang 2018.

653 **Lemma 8.** *Suppose Assumptions 1- 4 hold. Then, we have, for any $x, x' \in \mathbb{R}^p$,*

$$654 \quad \|\nabla\Phi(x) - \nabla\Phi(x')\| \leq L_\Phi \|x - x'\|,$$

655 *where the constant L_Φ is given by*

$$656 \quad L_\Phi = L + \frac{2L^2 + \tau M^2}{\mu} + \frac{\rho LM + L^3 + \tau ML}{\mu^2} + \frac{\rho L^2 M}{\mu^3}. \quad (12)$$

660 **A.1 PROOF OF LEMMA 1**
 661

662 **Proof.** By the update rule of y_k , we have for each $k = 1, \dots, K$,

$$663 \quad \begin{aligned} \|y_k^0 - \hat{y}_k\| &= \alpha \|\nabla_y g(x_k, y_k^0)\| = \alpha \|\nabla_y g(x_k, \hat{y}_{k-1})\| \\ 664 &= \alpha \|\nabla_y g(x_k, \hat{y}_{k-1}) - \nabla_y g(x_k, y_{k-1}^*) + \nabla_y g(x_k, y_{k-1}^*) - \nabla_y g(x_{k-1}, y_{k-1}^*)\| \\ 665 &\leq \alpha L (\|\hat{y}_{k-1} - y_{k-1}^*\| + \|x_{k-1} - x_k\|). \end{aligned}$$

666 The second conclusion holds that

$$667 \quad \begin{aligned} \|\hat{y}_k - y_k^*\| &\leq (1 - \mu\alpha) \|y_k^0 - y_k^*\| \leq (1 - \mu\alpha) \|\hat{y}_{k-1} - y_{k-1}^*\| + \|y_{k-1}^* - y_k^*\| \\ 668 &\stackrel{(i)}{\leq} (1 - \mu\alpha) \|\hat{y}_{k-1} - y_{k-1}^*\| + \frac{L}{\mu} \|x_{k-1} - x_k\|, \end{aligned}$$

669 where (i) follows from Lemma 2.2 in Ghadimi & Wang (2018). \square

670 **A.2 PROOF OF LEMMA 2**
 671

672 In the following two proofs, we will respectively present the two conclusions (Eq. (4) and Eq. (5))
 673 in Lemma 2.

674 **Proof.** According to the triangle inequality, we have $\|\hat{v}_k - v_k^*\| \leq \|\hat{v}_k - \tilde{v}_k^*\| + \|\tilde{v}_k^* - v_k^*\|$ for
 675 $k = 1, 2, \dots, K$. Then we focus on using $\|\hat{y}_k - y_k^*\|$ to bound $\|\tilde{v}_k^* - v_k^*\|$:

$$676 \quad \begin{aligned} \|\tilde{v}_k^* - v_k^*\| &= \|[\nabla_y^2 g(x_k, \hat{y}_k)]^{-1} \nabla_y f(x_k, \hat{y}_k) - [\nabla_y^2 g(x_k, y_k^*)]^{-1} \nabla_y f(x_k, y_k^*)\| \\ 677 &\leq \|[\nabla_y^2 g(x_k, \hat{y}_k)]^{-1} \nabla_y f(x_k, \hat{y}_k) - [\nabla_y^2 g(x_k, y_k^*)]^{-1} \nabla_y f(x_k, \hat{y}_k)\| \\ 678 &\quad + \|[\nabla_y^2 g(x_k, y_k^*)]^{-1} \nabla_y f(x_k, \hat{y}_k) - [\nabla_y^2 g(x_k, y_k^*)]^{-1} \nabla_y f(x_k, y_k^*)\| \\ 679 &\leq \|[\nabla_y^2 g(x_k, \hat{y}_k)]^{-1} - [\nabla_y^2 g(x_k, y_k^*)]^{-1}\| \cdot \|\nabla_y f(x_k, \hat{y}_k)\| \\ 680 &\quad + \|[\nabla_y^2 g(x_k, y_k^*)]^{-1}\| \cdot \|\nabla_y f(x_k, \hat{y}_k) - \nabla_y f(x_k, y_k^*)\| \\ 681 &\leq \frac{\rho M \|\hat{y}_k - y_k^*\|}{\mu^2} + \frac{L}{\mu} \|\hat{y}_k - y_k^*\| = \left(\frac{\rho M}{\mu^2} + \frac{L}{\mu} \right) \|\hat{y}_k - y_k^*\|. \end{aligned}$$

682 Then, we can get the conclusion of Eq. (4). \square

683 **Proof.** By the updated rule, we can obtain that

$$684 \quad \|\hat{v}_k - \tilde{v}_k^*\| \leq (1 - \mu\eta) \|v_k^0 - \tilde{v}_k^*\| \leq (1 - \mu\eta) \|\hat{v}_{k-1} - \tilde{v}_{k-1}^*\| + \|\tilde{v}_{k-1}^* - \tilde{v}_k^*\|.$$

685 For the second term $\|\tilde{v}_{k-1}^* - \tilde{v}_k^*\|$, we have

$$686 \quad \begin{aligned} \|\tilde{v}_{k-1}^* - \tilde{v}_k^*\| &= \|[\nabla_y^2 g(x_{k-1}, \hat{y}_{k-1})]^{-1} \nabla_y f(x_{k-1}, \hat{y}_{k-1}) - [\nabla_y^2 g(x_k, \hat{y}_k)]^{-1} \nabla_y f(x_k, \hat{y}_k)\| \\ 687 &\leq \|[\nabla_y^2 g(x_{k-1}, \hat{y}_{k-1})]^{-1} \nabla_y f(x_{k-1}, \hat{y}_{k-1}) - [\nabla_y^2 g(x_k, \hat{y}_k)]^{-1} \nabla_y f(x_{k-1}, \hat{y}_{k-1})\| \\ 688 &\quad + \|[\nabla_y^2 g(x_k, \hat{y}_k)]^{-1} \nabla_y f(x_{k-1}, \hat{y}_{k-1}) - [\nabla_y^2 g(x_k, \hat{y}_k)]^{-1} \nabla_y f(x_k, \hat{y}_k)\| \\ 689 &\leq \|[\nabla_y^2 g(x_{k-1}, \hat{y}_{k-1})]^{-1} - [\nabla_y^2 g(x_k, \hat{y}_k)]^{-1}\| \cdot \|\nabla_y f(x_{k-1}, \hat{y}_{k-1})\| \\ 690 &\quad + \|[\nabla_y^2 g(x_k, \hat{y}_k)]^{-1}\| \cdot \|\nabla_y f(x_{k-1}, \hat{y}_{k-1}) - \nabla_y f(x_k, \hat{y}_k)\|. \end{aligned}$$

702 Furthermore,
703

$$\begin{aligned}
 704 & \|\nabla_y f(x_{k-1}, \hat{y}_{k-1}) - \nabla_y f(x_k, \hat{y}_k)\| \\
 705 & \leq \|\nabla_y f(x_{k-1}, \hat{y}_{k-1}) - \nabla_y f(x_k, y_k^0)\| + \|\nabla_y f(x_k, y_k^0) - \nabla_y f(x_k, \hat{y}_k)\| \\
 706 & \leq L \|x_{k-1} - x_k\| + L \|y_k^0 - \hat{y}_k\|.
 \end{aligned}$$

708
709 Then, we have

$$\begin{aligned}
 710 & \|\nabla_y^2 g(x_{k-1}, \hat{y}_{k-1})^{-1} - \nabla_y^2 g(x_k, \hat{y}_k)^{-1}\| \cdot \|\nabla_y f(x_{k-1}, \hat{y}_{k-1})\| \\
 711 & \leq \|\nabla_y^2 g(x_{k-1}, \hat{y}_{k-1})^{-1}\| \|\nabla_y^2 g(x_{k-1}, \hat{y}_{k-1}) - \nabla_y^2 g(x_k, \hat{y}_k)\| \|\nabla_y^2 g(x_k, \hat{y}_k)^{-1}\| \\
 712 & \quad \cdot \|\nabla_y f(x_{k-1}, \hat{y}_{k-1})\| \\
 713 & \leq \frac{\rho (\|\hat{y}_{k-1} - \hat{y}_k\| + \|x_{k-1} - x_k\|)}{\mu^2} \|\nabla_y f(x_{k-1}, \hat{y}_{k-1})\| \\
 714 & \leq \frac{\rho M}{\mu^2} (\|\hat{y}_{k-1} - \hat{y}_k\| + \|x_{k-1} - x_k\|).
 \end{aligned}$$

719
720 Thus, we can obtain that

$$\begin{aligned}
 721 & \|\tilde{v}_{k-1}^* - \tilde{v}_k^*\| \leq \frac{\rho M (\|\hat{y}_{k-1} - \hat{y}_k\| + \|x_{k-1} - x_k\|)}{\mu^2} + \frac{L \|x_{k-1} - x_k\| + L \|y_k^0 - \hat{y}_k\|}{\mu} \\
 722 & = \left(\frac{\rho M}{\mu^2} + \frac{L}{\mu} \right) \|y_k^0 - \hat{y}_k\| + \left(\frac{\rho M}{\mu^2} + \frac{L}{\mu} \right) \|x_{k-1} - x_k\|.
 \end{aligned}$$

727 Then, we can get the conclusion of Eq. (5). □

729 730 A.3 PROOF OF LEMMA 3

731 **Proof.** According to the definition of the hypergradient, we have

$$\begin{aligned}
 732 & \|\widehat{\nabla} \Phi(x_k) - \nabla \Phi(x_k)\| = \|\nabla_x f(x_k, \hat{y}_k) - \nabla_{xy}^2 g(x_k, \hat{y}_k) \hat{v}_k - \nabla_x f(x_k, y_k^*) + \nabla_{xy}^2 g(x_k, y_k^*) v_k^*\| \\
 733 & \leq \|\nabla_x f(x_k, y_k^*) - \nabla_x f(x_k, \hat{y}_k)\| + \|\nabla_{xy}^2 g(x_k, \hat{y}_k) (v_k^* - \hat{v}_k)\| \\
 734 & \quad + \|(\nabla_{xy}^2 g(x_k, y_k^*) - \nabla_{xy}^2 g(x_k, \hat{y}_k)) v_k^*\| \\
 735 & \leq \left(L + \frac{\rho M}{\mu} \right) \|\hat{y}_k - y_k^*\| + L \|\hat{v}_k - v_k^*\| \\
 736 & \stackrel{Eq. (4)}{\leq} \left(L + \frac{\rho M}{\mu} + C_0 L \right) \|\hat{y}_k - y_k^*\| + L \|\hat{v}_k - v_k^*\|.
 \end{aligned}$$

743
744 Then, the proof is completed. □

745 746 A.4 PROOF OF LEMMA 4

747
748 **Proof.** Firstly, we have

$$\begin{aligned}
 749 & \|\hat{v}_k - \tilde{v}_k^*\| \leq (1 - \mu\eta) \|\hat{v}_{k-1} - \tilde{v}_{k-1}^*\| + C_0 \|y_k^0 - \hat{y}_k\| + \left(\frac{\rho M}{\mu^2} + \frac{L}{\mu} \right) \|x_{k-1} - x_k\| \\
 750 & \stackrel{Eq. (2)}{\leq} (1 - \mu\eta) \|\hat{v}_{k-1} - \tilde{v}_{k-1}^*\| + C_0 \alpha L \|\hat{y}_{k-1} - y_{k-1}^*\| \\
 751 & \quad + \left(\frac{\alpha L^2 C_0}{\mu} + \frac{\rho M}{\mu^2} + \frac{L}{\mu} \right) \|x_{k-1} - x_k\|.
 \end{aligned}$$

756 Then we have

$$\begin{aligned}
& \| \hat{v}_k - \tilde{v}_k^* \| + C_1 \| \hat{y}_k - y_k^* \| \\
& \leq (1 - \mu\eta) \| \hat{v}_{k-1} - \tilde{v}_{k-1}^* \| + C_0\alpha L \| \hat{y}_{k-1} - y_{k-1}^* \| + \left(\frac{\alpha L^2 C_0}{\mu} + \frac{\rho M}{\mu^2} + \frac{L}{\mu} \right) \| x_{k-1} - x_k \| \\
& \quad + (1 - \mu\alpha) C_1 \| \hat{y}_{k-1} - y_{k-1}^* \| + \frac{LC_1}{\mu} \| x_{k-1} - x_k \| \\
& = (1 - \mu\eta) \| \hat{v}_{k-1} - \tilde{v}_{k-1}^* \| + \left(1 - \mu\alpha + \frac{C_0\alpha L}{C_1} \right) \cdot C_1 \| \hat{y}_{k-1} - y_{k-1}^* \| \\
& \quad + \left(\frac{\alpha L^2 C_0}{\mu} + \frac{\rho M}{\mu^2} + \frac{L}{\mu} + \frac{LC_1}{\mu} \right) \| x_{k-1} - x_k \|.
\end{aligned}$$

769 By the update rule of $\{x_k\}$, we can obtain that

$$\begin{aligned}
770 \| x_{k-1} - x_k \| &= \beta \| \hat{\nabla} \Phi(x_{k-1}) \| \leq \beta \| \nabla \Phi(x_{k-1}) \| + \beta \| \hat{\nabla} \Phi(x_{k-1}) - \nabla \Phi(x_{k-1}) \| \\
771 &\stackrel{Eq. (6)}{\leq} \beta \| \nabla \Phi(x_{k-1}) \| + \beta \left(L + \frac{\rho M}{\mu} + C_0 L \right) \| \hat{y}_{k-1} - y_{k-1}^* \| + \beta L \| \hat{v}_{k-1} - \tilde{v}_{k-1}^* \|.
\end{aligned}$$

775 Thus, we have

$$\begin{aligned}
776 \| \hat{v}_k - \tilde{v}_k^* \| + C_1 \| \hat{y}_k - y_k^* \| \\
777 &\leq \left(1 - \mu\eta + \beta L \left(\frac{\alpha L^2 C_0}{\mu} + \frac{\rho M}{\mu^2} + \frac{L}{\mu} + \frac{LC_1}{\mu} \right) \right) \| \hat{v}_{k-1} - \tilde{v}_{k-1}^* \| \\
778 &\quad + \left(1 - \mu\alpha + \frac{C_0\alpha L}{C_1} + \frac{\beta}{C_1} \left(L + \frac{\rho M}{\mu} + C_0 L \right) \left(\frac{\alpha L^2 C_0}{\mu} + \frac{\rho M}{\mu^2} + \frac{L}{\mu} + \frac{LC_1}{\mu} \right) \right) \\
779 &\quad \cdot C_1 \| \hat{y}_{k-1} - y_{k-1}^* \| + \beta \left(\frac{\alpha L^2 C_0}{\mu} + \frac{\rho M}{\mu^2} + \frac{L}{\mu} + \frac{LC_1}{\mu} \right) \| \nabla \Phi(x_{k-1}) \|.
\end{aligned}$$

785 We denote that $C_2 = \frac{\alpha L^2 C_0}{\mu} + \frac{\rho M}{\mu^2} + \frac{L}{\mu} + \frac{LC_1}{\mu}$ and $C_3 = L + \frac{\rho M}{\mu} + C_0 L$. Then the above equation
786 can rewrite as follows

$$\begin{aligned}
787 \| \hat{v}_k - \tilde{v}_k^* \| + C_1 \| \hat{y}_k - y_k^* \| \\
788 &\leq (1 - \mu\eta + \beta L C_2) \| \hat{v}_{k-1} - \tilde{v}_{k-1}^* \| + \left(1 - \mu\alpha + \frac{C_0\alpha L}{C_1} + \frac{\beta C_2 C_3}{C_1} \right) \cdot C_1 \| \hat{y}_{k-1} - y_{k-1}^* \| \\
789 &\quad + \beta C_2 \| \nabla \Phi(x_{k-1}) \|.
\end{aligned}$$

794 We only need to $1 - \mu\eta + \beta L C_2 \leq 1 - \frac{\mu\eta}{2}$, $\frac{C_0\alpha L}{C_1} = \frac{\mu\alpha}{4}$ and $\frac{\beta C_2 C_3}{C_1} \leq \frac{\mu\alpha}{4}$. Then we can get

$$\begin{aligned}
795 \beta &\leq \frac{\eta\mu}{2LC_2}, \quad \beta \leq \frac{C_1\mu\alpha}{4C_2C_3}, \quad C_1 = \frac{4C_0L}{\mu}, \\
796 C_2 &= \left(\frac{\alpha L^2 C_0}{\mu} + \frac{\rho M}{\mu^2} + \frac{L}{\mu} + \frac{LC_1}{\mu} \right) \stackrel{\alpha=\frac{1}{L}}{=} \frac{4L^3}{\mu^3} + \frac{4L^2\rho M}{\mu^4} + \frac{L^2}{\mu^2} + \frac{L\rho M}{\mu^3} + \frac{L}{\mu} + \frac{\rho M}{\mu^2}, \\
797 C_3 &= L + \frac{\rho M}{\mu} + C_0 L = L + \frac{\rho M}{\mu} + \frac{\rho M L}{\mu^2} + \frac{L^2}{\mu}.
\end{aligned}$$

803 Then, we have

$$\begin{aligned}
804 \beta &\leq \frac{C_1\mu\alpha}{4C_2C_3} = \frac{\mu^4(\rho M + L\mu)}{(4L^3\mu + 4L^2\rho M + 2L^2\mu^2 + 2L\mu\rho M + L\mu^3)(L\mu^2 + \rho M\mu + \rho M L + L^2\mu)} \\
805 &\quad = \mathcal{O}(\kappa^{-4}), \\
806 \beta &\leq \frac{\eta\mu}{2LC_2} \stackrel{\eta=\frac{1}{L}}{=} \frac{\mu^5}{2L^2(4L^3\mu + 4L^2\rho M + L^2\mu^2 + L\mu\rho M + L\mu^3)} = \mathcal{O}(\kappa^{-5}).
\end{aligned}$$

810 Then, we have $\beta \leq \min\{\mathcal{O}(\kappa^{-4}), \mathcal{O}(\kappa^{-5})\} = \mathcal{O}(\kappa^{-5})$. Thus, we have

$$\begin{aligned} 811 \quad & \|\hat{v}_k - \tilde{v}_k^*\| + C_1 \|\hat{y}_k - y_k^*\| \\ 812 \quad & \leq \max\left\{1 - \frac{\mu\eta}{2}, 1 - \frac{\alpha\mu}{2}\right\} \cdot (\|\hat{v}_{k-1} - \tilde{v}_{k-1}^*\| + C_1 \|\hat{y}_{k-1} - y_{k-1}^*\|) + \beta C_2 \|\nabla\Phi(x_{k-1})\| \\ 813 \quad & = \left(1 - \frac{\mu}{2L}\right) \cdot (\|\hat{v}_{k-1} - \tilde{v}_{k-1}^*\| + C_1 \|\hat{y}_{k-1} - y_{k-1}^*\|) + \beta C_2 \|\nabla\Phi(x_{k-1})\| \\ 814 \quad & \\ 815 \quad & \\ 816 \end{aligned}$$

817 Accordingly, we have

$$\begin{aligned} 818 \quad & (\|\hat{v}_k - \tilde{v}_k^*\| + C_1 \|\hat{y}_k - y_k^*\|)^2 \leq \left(1 - \frac{\mu}{4L}\right) \cdot (\|\hat{v}_{k-1} - \tilde{v}_{k-1}^*\| + C_1 \|\hat{y}_{k-1} - y_{k-1}^*\|)^2 \\ 819 \quad & \quad + \frac{3\beta^2 C_2^2 L}{\mu} \|\nabla\Phi(x_{k-1})\|^2. \\ 820 \quad & \\ 821 \quad & \\ 822 \end{aligned}$$

823 Moreover, we have

$$\begin{aligned} 824 \quad & \|\hat{v}_k - \tilde{v}_k^*\| + C_1 \|\hat{y}_k - y_k^*\| \leq \left(1 - \frac{\mu}{2L}\right)^k \cdot \left(\|v_0^Q - \tilde{v}_0^*\| + C_1 \|y_0^N - y_0^*\|\right) \\ 825 \quad & \quad + \beta C_2 \sum_{t=0}^k \left(1 - \frac{\mu}{2L}\right)^{k-1-t} \|\nabla\Phi(x_t)\|. \\ 826 \quad & \\ 827 \quad & \\ 828 \quad & \\ 829 \end{aligned}$$

Thus, we can obtain that

$$\begin{aligned} 830 \quad & (\|\hat{v}_k - \tilde{v}_k^*\| + C_1 \|\hat{y}_k - y_k^*\|)^2 \leq \left(1 - \frac{\mu}{4L}\right)^k \cdot \left(\|v_0^Q - \tilde{v}_0^*\| + C_1 \|y_0^N - y_0^*\|\right)^2 \\ 831 \quad & \quad + \frac{3\beta^2 C_2^2 L}{\mu} \sum_{t=0}^k \left(1 - \frac{\mu}{4L}\right)^{k-1-t} \|\nabla\Phi(x_t)\|^2. \quad (13) \\ 832 \quad & \\ 833 \quad & \\ 834 \quad & \\ 835 \end{aligned}$$

Therefore, we have

$$\begin{aligned} 836 \quad & \|\hat{\nabla}\Phi(x_k) - \nabla\Phi(x_k)\|^2 \leq L^2 \left(\|\hat{v}_k - \tilde{v}_k^*\| + \frac{C_3}{L} \|\hat{y}_k - y_k^*\|\right)^2 \\ 837 \quad & \leq L^2 (\|\hat{v}_k - \tilde{v}_k^*\| + C_1 \|\hat{y}_k - y_k^*\|)^2 \\ 838 \quad & \leq L^2 \left(1 - \frac{\mu}{4L}\right)^k \cdot \left(\|v_0^Q - \tilde{v}_0^*\| + C_1 \|y_0^N - y_0^*\|\right)^2 \\ 839 \quad & \quad + \frac{3\beta^2 C_2^2 L^3}{\mu} \sum_{t=0}^k \left(1 - \frac{\mu}{4L}\right)^{k-1-t} \|\nabla\Phi(x_t)\|^2, \\ 840 \quad & \\ 841 \quad & \\ 842 \quad & \\ 843 \quad & \\ 844 \quad & \\ 845 \quad & \\ 846 \end{aligned}$$

where the second inequality is because of $C_3 \leq LC_1$ and the specific derivation process is as follows

$$\frac{C_3}{LC_1} = \frac{\mu(L+\mu)}{L^2} = \frac{1}{\kappa} + \frac{1}{\kappa^2} < 1,$$

where $C_3 = \frac{(L\mu+\rho M)\cdot(L+\mu)}{\mu^2}$ and $LC_1 = \frac{L^2(L\mu+\rho M)}{\mu^3}$. \square

A.5 PROOF OF THEOREM 1

853 **Proof.** First, based on Lemma 2 in Ji et al. (2021), we have $\nabla\Phi(\cdot)$ is L_Φ -Lipschitz, where $L_\Phi =$
854 $L + \frac{2L^2+\rho M^2}{\mu} + \frac{2\rho LM+L^3}{\mu^2} + \frac{\rho L^2 M}{\mu^3} = \Theta(\kappa^3)$. Then, we have

$$\begin{aligned} 855 \quad & \Phi(x_{k+1}) \leq \Phi(x_k) + \langle \nabla\Phi(x_k), x_{k+1} - x_k \rangle + \frac{L_\Phi}{2} \|x_{k+1} - x_k\|^2 \\ 856 \quad & \leq \Phi(x_k) - \left(\frac{\beta}{2} - \beta^2 L_\Phi\right) \|\nabla\Phi(x_k)\|^2 + \left(\frac{\beta}{2} + \beta^2 L_\Phi\right) \|\nabla\Phi(x_k) - \hat{\nabla}\Phi(x_k)\|^2 \\ 857 \quad & \stackrel{Eq. (7)}{\leq} \Phi(x_k) - \left(\frac{\beta}{2} - \beta^2 L_\Phi\right) \|\nabla\Phi(x_k)\|^2 + \left(\frac{\beta}{2} + \beta^2 L_\Phi\right) L^2 \left(1 - \frac{\mu}{4L}\right)^k \cdot \\ 858 \quad & \quad \left(\|v_0^Q - \tilde{v}_0^*\| + C_1 \|y_0^N - y_0^*\|\right)^2 + \left(\frac{\beta}{2} + \beta^2 L_\Phi\right) \frac{3\beta^2 C_2^2 L^3}{\mu} \sum_{t=0}^k \left(1 - \frac{\mu}{4L}\right)^{k-1-t} \|\nabla\Phi(x_t)\|^2. \\ 859 \quad & \\ 860 \quad & \\ 861 \quad & \\ 862 \quad & \\ 863 \quad & \\ 864 \quad & \\ 865 \end{aligned}$$

864 Telescoping above equation over k from 0 to $K - 1$, we can obtain that
 865

$$\begin{aligned}
 866 \quad \Phi(x_{K-1}) &\leq \Phi(x_0) - \left(\frac{\beta}{2} - \beta^2 L_\Phi\right) \sum_{k=0}^{K-1} \|\nabla \Phi(x_k)\|^2 + \left(\frac{\beta}{2} + \beta^2 L_\Phi\right) \frac{4L^3}{\mu} \\
 867 \quad &\cdot \left(\|v_0^Q - \tilde{v}_0^*\| + C_1 \|y_0^N - y_0^*\|\right)^2 + \left(\frac{\beta}{2} + \beta^2 L_\Phi\right) \frac{12\beta^2 C_2^2 L^4}{\mu^2} \sum_{k=0}^{K-1} \|\nabla \Phi(x_k)\|^2 \\
 868 \quad &= \Phi(x_0) - \beta \left(\frac{1}{2} - \beta L_\Phi - \left(\frac{1}{2} + \beta L_\Phi\right) \frac{12\beta^2 C_2^2 L^4}{\mu^2}\right) \sum_{k=0}^{K-1} \|\nabla \Phi(x_k)\|^2 \\
 869 \quad &\quad + \left(\frac{\beta}{2} + \beta^2 L_\Phi\right) \frac{4L^3}{\mu} \cdot \left(\|v_0^Q - \tilde{v}_0^*\| + C_1 \|y_0^N - y_0^*\|\right)^2.
 \end{aligned}$$

870 Because $\beta = \min\{\frac{1}{8L_\Phi} = \mathcal{O}(\kappa^{-3}), \mathcal{O}(\kappa^{-5})\} = \mathcal{O}(\kappa^{-5})$, we can obtain that
 871

$$\frac{1}{K} \sum_{k=0}^{K-1} \|\nabla \Phi(x_k)\|^2 \leq \frac{\Phi(x_0) - \Phi(x^*)}{\beta AK} + \frac{4L^3(1+2\beta L_\Phi)}{2\mu AK} \cdot \left(\|v_0^Q - \tilde{v}_0^*\| + C_1 \|y_0^N - y_0^*\|\right)^2,$$

872 where $A = \frac{1}{2} - \beta L_\Phi - \left(\frac{1}{2} + \beta L_\Phi\right) \frac{12\beta^2 C_2^2 L^4}{\mu^2}$, $L_\Phi = L + \frac{2L^2 + \rho M^2}{\mu} + \frac{2\rho LM + L^3}{\mu^2} + \frac{\rho L^2 M}{\mu^3} = \mathcal{O}(\kappa^3)$.
 873

874 We rewrite y_0^N as $y_0^{N_0}$ and Let $N_0 \geq \frac{\ln(\mu)}{\ln(\mu/(\mu-L))}$, Thus, we have
 875

$$\|v_0^Q - \tilde{v}_0^*\| + C_1 \|y_0^N - y_0^*\| \leq \frac{M}{\mu} + \frac{2}{\mu}(L \|y_0^*\| + M) + 4L \left(\frac{\rho M}{\mu^2} + \frac{L}{\mu}\right) \|y_0^*\| = \mathcal{O}(\kappa^2),$$

876 because $\|y_0^{N_0} - y_0^*\| \leq (1 - \alpha\mu)^{N_0} \|y_0^0 - y_0^*\| \leq \mu \|y_0^*\|$. For the first term, we have
 877

$$\frac{\Phi(x_0) - \Phi(x^*)}{\beta A} = \frac{2\mu^2(\Phi(x_0) - \Phi(x^*))}{\beta\mu^2 - 2\beta^2 L_\Phi - 12\beta^3 C_2^2 L^4 - 24\beta^4 L_\Phi C_2^2 L^4} = \mathcal{O}(\kappa^5).$$

878 For the second term, we have
 879

$$\begin{aligned}
 880 \quad &\frac{4L^3(1+2\beta L_\Phi)}{2\mu AK} \cdot \left(\|v_0^Q - \tilde{v}_0^*\| + C_1 \|y_0^N - y_0^*\|\right)^2 \\
 881 \quad &= \frac{4L^3\mu + 8\beta L_\Phi L^3\mu}{(1 - 2\beta L_\Phi)\mu^2 - 12\beta^2 C_2^2 L^4(1 + 2\beta L_\Phi)} \cdot \left(\|v_0^Q - \tilde{v}_0^*\| + C_1 \|y_0^N - y_0^*\|\right)^2 = \mathcal{O}(\kappa^5).
 \end{aligned}$$

882 Then, we have
 883

$$\frac{1}{K} \sum_{k=0}^{K-1} \|\nabla \Phi(x_k)\|^2 = \mathcal{O}\left(\frac{\kappa^5}{K} + \frac{\kappa^5}{K}\right) = \mathcal{O}\left(\frac{\kappa^5}{K}\right).$$

884 Then, to achieve an ϵ -accurate stationary point, we have $K = \mathcal{O}(\kappa^5 \epsilon^{-1})$, and hence we have the
 885 following complexity results. 1) Gradient complexity: $\text{Gc}(\epsilon) = 3K = \tilde{\mathcal{O}}(\kappa^5 \epsilon^{-1})$. 2) Matrix-vector
 886 product complexities: $\text{Mv}(\epsilon) = K + KQ = \tilde{\mathcal{O}}(\kappa^5 \epsilon^{-1})$. \square
 887

909 B PROOFS OF THE SINGLE-LOOP ITD-BASED ALGORITHM

910 B.1 ADDITIONAL USEFUL LEMMA

911 **Lemma 9.** Consider the single-loop ITD-based algorithm in Algorithm 2. Suppose Assumptions
 912 1-4 hold. Let $\alpha \leq \frac{1}{L}$, we have
 913

$$\| \nabla_x y_k^N(x_k) - \nabla_x y_k^*(x_k) \| \leq (1 - \alpha\mu) \| \nabla_x y^*(x_k) \| + \alpha\rho \| y_k^0 - y^*(x_k) \|,$$

914 where $y_k^N(x_k) = y_k^0 - \alpha \nabla_y g(x_k, y_k^0)$ and $y_k^* = \arg \min_y g(x_k, y)$ for $k = 1, \dots, K$.
 915

Proof. According to the definition, we have $\nabla_{xy}y_k^N(x_k) = -\alpha\nabla_{xy}^2g(x_k, y_k^0)$ and $\nabla_{xy}^*(x_k) = -[\nabla_{yy}^2g(x_k, y_k^*)]^{-1}\nabla_{xy}^2g(x_k, y_k^*)$. Thus, we have

$$\begin{aligned}
\|\nabla_x y_k^N(x_k) - \nabla_x y_k^*(x_k)\| &= \|-\alpha \nabla_{xy}^2 g(x_k, y_k^0) + [\nabla_{yy}^2 g(x_k, y_k^*)]^{-1} \nabla_{xy}^2 g(x_k, y_k^*)\| \\
&\leq \|(I - \alpha \nabla_{yy}^2 g(x_k, y_k^*)) [\nabla_{yy}^2 g(x_k, y_k^*)]^{-1} \nabla_{xy}^2 g(x_k, y_k^*)\| \\
&\quad + \|\alpha (\nabla_{xy}^2 g(x_k, y_k^*) - \nabla_{xy}^2 g(x_k, y_k^0))\| \\
&\leq (1 - \alpha\mu) \|\nabla_x y^*(x_k)\| + \alpha\rho \|y_k^0 - y^*(x_k)\|.
\end{aligned}$$

Then, the proof is completed.

B.2 PROOF OF LEMMA 5

Proof. Accordingly, we have

$$\begin{aligned}
\|\hat{y}_k - y^*(x_k)\| &\leq (1 - \mu\alpha) \|\hat{y}_{k-1} - y^*(x_{k-1})\| + \frac{L}{\mu} \|x_{k-1} - x_k\| \\
&\leq (1 - \mu\alpha) \|\hat{y}_{k-1} - y^*(x_{k-1})\| + \frac{L\beta}{\mu} \|\hat{\nabla}\Phi(x_{k-1})\| \\
&\leq (1 - \mu\alpha) \|\hat{y}_{k-1} - y^*(x_{k-1})\| + \frac{L\beta}{\mu} \left(\|\nabla\Phi(x_{k-1})\| + \|\hat{\nabla}\Phi(x_{k-1}) - \nabla\Phi(x_{k-1})\| \right) \\
&\leq (1 - \mu\alpha) \|\hat{y}_{k-1} - y^*(x_{k-1})\| + \frac{L\beta}{\mu} (\|\nabla\Phi(x_{k-1})\| + C_4 \|\hat{y}_{k-1} - y_{k-1}^*\| + C_5) \\
&\leq \left(1 - \mu\alpha + \frac{L\beta C_4}{\mu} \right) \|\hat{y}_{k-1} - y^*(x_{k-1})\| + \frac{L\beta}{\mu} \|\nabla\Phi(x_{k-1})\| + \frac{L\beta C_5}{\mu}.
\end{aligned}$$

We rewrite the above equation as $\|\hat{y}_k - y^*(x_k)\| \leq C_6 \|\hat{y}_{k-1} - y^*(x_{k-1})\| + \frac{L\beta}{\mu} \|\nabla \Phi(x_{k-1})\| + C_7$, where $C_6 = 1 - \mu\alpha + \frac{L\beta C_4}{\mu}$ and $C_7 = \frac{L\beta C_5}{\mu}$. Then, the proof of Eq. (8) is completed.

Since $\beta \leq \frac{\mu^3}{2L(2L^2+\rho M)}$, we have $C_6 \leq 1 - \frac{\mu}{2L}$. Accordingly, we have

$$\|\hat{y}_k - y^*(x_k)\| \leq \left(1 - \frac{\mu}{2L}\right)^k \|\hat{y}_0 - y^*(x_0)\| + \frac{L\beta^2}{\mu} \sum_{j=0}^{k-1} \left(1 - \frac{\mu}{2L}\right)^{k-1-j} (\|\nabla\Phi(x_j)\| + C_5).$$

Then, the proof of Eq. (9) is completed. Similar with AID in Eq. (13), we can obtain

$$\|\hat{y}_k - y^*(x_k)\|^2 \leq \left(1 - \frac{\mu}{4L}\right)^k \|\hat{y}_0 - y^*(x_0)\|^2 + \frac{3L\beta^2}{\mu} \sum_{j=0}^{k-1} \left(1 - \frac{\mu}{4L}\right)^{k-1-j} (\|\nabla\Phi(x_j)\| + C_5)^2. \quad (14)$$

B.3 PROOF OF LEMMA 6

Proof. First, according to the definition of $\hat{\nabla}\Phi(x_k)$ and $\nabla\Phi(x_k)$, we have

$$\begin{aligned}
& \left\| \widehat{\nabla} \Phi(x_k) - \nabla \Phi(x_k) \right\| \\
& \leq \left\| \nabla_1 f(x_k, \hat{y}_k) + \nabla_x \hat{y}_k(x_k) \nabla_2 f(x_k, \hat{y}_k) - \nabla_1 f(x_k, y_k^*) - \nabla_x y_k^*(x_k) \nabla_2 f(x_k, y_k^*) \right\| \\
& \leq L \left\| \hat{y}_k - y_k^* \right\| + \left\| \nabla_x \hat{y}_k(x_k) \nabla_2 f(x_k, \hat{y}_k) - \nabla_x \hat{y}_k(x_k) \nabla_2 f(x_k, y_k^*) \right\| \\
& \quad + \left\| \nabla_x \hat{y}_k(x_k) \nabla_2 f(x_k, y_k^*) - \nabla_x y_k^*(x_k) \nabla_2 f(x_k, y_k^*) \right\| \\
& \leq L \left\| \hat{y}_k - y_k^* \right\| + \alpha L^2 \left\| \hat{y}_k - y_k^* \right\| + M \left((1 - \alpha\mu) \frac{L}{\mu} + \alpha\rho \left\| y_k^0 - y_k^* \right\| \right).
\end{aligned}$$

For the relationship of $\|y_k^0 - y^*(x_k)\|$ and $\|\hat{y}_k - y^*(x_k)\|$, we have

$$\|y_k^0 - y^*(x_k)\| \leq \alpha \|\nabla_y g(x_k, y_k^0)\| + \|\hat{y}_k - y^*(x_k)\| \leq \alpha M + \|\hat{y}_k - y^*(x_k)\|.$$

Then, we have

$$\left\| \widehat{\nabla} \Phi(x_k) - \nabla \Phi(x_k) \right\| \leq C_4 \left\| \hat{y}_k - y_k^* \right\| + C_5, \quad (15)$$

where $C_4 \equiv L + \alpha L^2 + \alpha \rho M$ and $C_5 \equiv M(1 - \alpha \mu) \frac{L}{\alpha} + \alpha^2 \rho M^2$.

972 B.4 PROOF OF LEMMA 7
973974 **Proof.** According to Lemma 6, we have
975

976
$$\begin{aligned} \|\hat{\nabla}\Phi(x_k) - \nabla\Phi(x_k)\|^2 &\leq (C_4 \|\hat{y}_k - y_k^*\| + C_5)^2 \leq 2C_4^2 \|\hat{y}_k - y_k^*\|^2 + 2C_5^2 \\ 977 &\leq 2C_4^2 \left(1 - \frac{\mu}{4L}\right)^k \|\hat{y}_0 - y_0^*\|^2 + \frac{6L\beta^2 C_4^2}{\mu} \sum_{j=0}^{k-1} \left(1 - \frac{\mu}{4L}\right)^{k-1-j} (\|\nabla\Phi(x_j)\| + C_5)^2 + 2C_5^2, \end{aligned}$$

980

981 where the last inequality holds since Eq. (14). \square
982983 B.5 PROOF OF THEOREM 3
984985 **Proof.** First, based on Lemma 2 in Ji et al. (2021), we have $\nabla\Phi(\cdot)$ is L_Φ -Lipschitz, where $L_\Phi =$
986 $L + \frac{2L^2 + \rho M^2}{\mu} + \frac{2\rho LM + L^3}{\mu^2} + \frac{\rho L^2 M}{\mu^3} = \Theta(\kappa^3)$. Then, we have
987

988
$$\begin{aligned} \Phi(x_{k+1}) &\leq \Phi(x_k) - \left(\frac{\beta}{2} - \beta^2 L_\Phi\right) \|\nabla\Phi(x_k)\|^2 + \left(\frac{\beta}{2} + \beta^2 L_\Phi\right) \|\hat{\nabla}\Phi(x_k) - \nabla\Phi(x_k)\|^2 \\ 989 &\leq \Phi(x_k) - \left(\frac{\beta}{2} - \beta^2 L_\Phi\right) \|\nabla\Phi(x_k)\|^2 + \left(\frac{\beta}{2} + \beta^2 L_\Phi\right) 2C_4^2 \left(1 - \frac{\mu}{4L}\right)^k \|\hat{y}_0 - y_0^*\|^2 \\ 990 &\quad + \left(\frac{\beta}{2} + \beta^2 L_\Phi\right) \frac{6L\beta^2 C_4^2}{\mu} \sum_{j=0}^{k-1} \left(1 - \frac{\mu}{4L}\right)^{k-1-j} (\|\nabla\Phi(x_j)\| + C_5)^2 + \left(\frac{\beta}{2} + \beta^2 L_\Phi\right) 2C_5^2. \end{aligned}$$

991

992 Telescoping the above equation over k from 0 to $K - 1$ yields
993

994
$$\begin{aligned} \Phi(x_{K-1}) &\leq \Phi(x_0) - \left(\frac{\beta}{2} - \beta^2 L_\Phi\right) \sum_{k=0}^{K-1} \|\nabla\Phi(x_k)\|^2 + \left(\frac{\beta}{2} + \beta^2 L_\Phi\right) C_4^2 \frac{8L}{\mu} \|\hat{y}_0 - y_0^*\|^2 \\ 995 &\quad + \left(\frac{\beta}{2} + \beta^2 L_\Phi\right) \frac{6L\beta^2 C_4^2}{\mu} \frac{4L}{\mu} \sum_{k=0}^{K-1} (\|\nabla\Phi(x_k)\| + C_5)^2 + \left(\frac{\beta}{2} + \beta^2 L_\Phi\right) 2C_5^2 K \\ 996 &\leq \Phi(x_0) - A \sum_{k=0}^{K-1} \|\nabla\Phi(x_k)\|^2 + B_1 + B_2 + \left(\frac{\beta}{2} + \beta^2 L_\Phi\right) 2C_5^2 K, \end{aligned}$$

997

998 where
999

1000
$$\begin{aligned} A &= \left(\frac{\beta}{2} - \beta^2 L_\Phi\right) - \left(\frac{\beta}{2} + \beta^2 L_\Phi\right) \frac{48L^2\beta^2 C_4^2}{\mu^2}, & B_1 &= \left(\frac{\beta}{2} + \beta^2 L_\Phi\right) C_4^2 \frac{8L}{\mu} \|\hat{y}_0 - y_0^*\|^2, \\ 1001 B_2 &= \left(\frac{\beta}{2} + \beta^2 L_\Phi\right) \frac{48L^2\beta^2 C_4^2 C_5^2}{\mu^2}. \end{aligned}$$

1002

1003 Thus we have
1004

1005
$$\frac{1}{K} \sum_{k=0}^{K-1} \|\nabla\Phi(x_k)\|^2 \leq \frac{\Phi(x_0) - \Phi(x^*)}{AK} + \frac{B_1 + B_2}{AK} + \left(\frac{\beta}{2} + \beta^2 L_\Phi\right) \frac{2C_5^2}{A},$$

1006

1007 where $\beta = \mathcal{O}(\kappa^{-3})$, $L_\Phi = \mathcal{O}(\kappa^3)$, $C_4 = \mathcal{O}(1)$, $C_5 = \mathcal{O}(\kappa^1)$. Thus we have $\frac{1}{A} = \mathcal{O}(\kappa^3)$,
1008 $\frac{B_1}{A} = \mathcal{O}(\kappa^1)$, $\frac{B_2}{A} = \mathcal{O}(\kappa^{-2})$. Therefore, we have
1009

1010
$$\frac{1}{K} \sum_{k=0}^{K-1} \|\nabla\Phi(x_k)\|^2 = \mathcal{O}\left(\frac{\kappa^3}{K} + \kappa^2\right).$$

1011

1012 Therefore the proof is completed. \square
10131024 C EXTENSION: APPLYING THE PROPOSED TECHNIQUE TO
1025 GRADIENT-BASED FIRST-ORDER METHODS

1026 **Algorithm 3** F²SA ($x_0, y_0, \beta, \alpha, \lambda, T$)

```

1027 1:  $z_0 = y_0$ 
1028 2: for  $t = 0, 1, \dots, T - 1$ 
1029 3:    $y_t^0 = y_t, z_t^0 = z_t$ 
1030 4:    $\hat{z}_t = z_t^0 - \alpha \nabla_y g(x_t, z_t^k)$ 
1031 5:    $\hat{y}_t = y_t^0 - \alpha (\nabla_y f(x_t, y_t^0) + \lambda \nabla_y g(x_t, y_t^0))$ 
1032 6:    $\hat{\nabla} \Phi(x_t) = \nabla_x f(x_t, \hat{y}_t) + \lambda (\nabla_x g(x_t, \hat{y}_t) - \nabla_x g(x_t, \hat{z}_t))$ 
1033 7:    $x_{t+1} = x_t - \beta \hat{\nabla} \Phi(x_t)$ 
1034 8: end for
1035
1036
1037
1038
```

1039 To verify the scalability of the proposed analytical technique, we consider the F²SA algorithm
1040 (Kwon et al., 2023a) in Algorithm 3, a gradient-based first-order method. Instead of directly studying
1041 the original hyper-objective $\Phi(x)$, this method studied the following value-function penalized
1042 hyper-objective as a bridge:

$$1043 \Phi_\lambda(x) := \min_y \{f(x, y) + \lambda(g(x, y) - g^*(x))\}, \quad (16)$$

$$1044$$

1045 where $g^*(x) = \min_y g(x, y)$ is the inner-level value-function. Before give the main result, we
1046 will describe the considered case for F²SA. Following Kwon et al. (2023a); Chen et al. (2024), we
1047 formally present the definition only for F²SA and these standard assumptions.

1048 **Definition 2** (Chen et al. (2024)). *We say x is an ϵ -first-order stationary point of a differentiable
1049 function $\varphi(x)$ if $\|\nabla \varphi(x)\| \leq \epsilon$.*

1050 **Assumption 5.** *Recall the bilevel problem defined in Equation 1, where f is the outer-level problem,
1051 g is the inner-level problem. Suppose that*

- 1053 1. *The inner-level function $g(x, y)$ is M -Lipschitz for z , where $z = (x, y)$;*
- 1054 2. *The outer-level function $f(x, y)$ has ρ -Lipschitz Hessians in y , i.e. $\nabla_{xy}^2 f$ and $\nabla_{yy}^2 f$ are
1055 ρ -Lipschitz continuous.*

1058 Assumption 5, together with Assumptions 1-4, constitutes the set of assumptions used by Kwon
1059 et al. (2023b) in their convergence analysis of F²SA; therefore, we adopt the same assumptions in
1060 our work. Under these assumptions, we define the condition number $\kappa := L/\mu$. Next, we will
1061 present some useful lemmas.

1062 **Lemma 10.** *Let $y_\lambda^* := \arg \min_{y \in \mathbb{R}^{d_y}} h_\lambda(x, y)$ denote the set of minima for the penalty function
1063 $h_\lambda(x, y) = f(x, y) + \lambda(g(x, y) - g^*(x))$. Under Assumptions 1-5, for $\lambda_2 \geq \lambda_1 \geq 2L/\mu$, we have
1064 that*

$$1065 \|\mathbf{y}_{\lambda_1}^*(x_1) - \mathbf{y}_{\lambda_2}^*(x_2)\| \leq \frac{2L}{\mu} |1/\lambda_1 - 1/\lambda_2| + \frac{3L}{\mu} \|x_1 - x_2\|.$$

$$1066$$

$$1067$$

1068 **Lemma 11** (Shen & Chen (2023)). *Recall that $\Phi_\lambda(x)$ is the penalized hyper-objective defined in
1069 Equation 16. Under Assumptions 1-5, $\nabla \Phi_\lambda(x)$ exists and takes the form of*

$$1070 \nabla \Phi_\lambda(x) = \nabla_x f(x, y_\lambda^*(x)) + \lambda(\nabla_x g(x, y_\lambda^*(x)) - \nabla_x g(x, y^*(x))). \quad (17)$$

$$1071$$

1072 **Lemma 12** (Chen et al. (2024)). *Under Assumptions 1-5, $\Phi(x)$ has $\mathcal{O}(\kappa^3)$ -Lipschitz gradients.*

1073 **Lemma 13** (Kwon et al. (2023b)). *Under Assumptions 1-5, according to the definition of $\nabla \Phi(x)$
1074 and $\nabla \Phi_\lambda(x)$. Let $\lambda > 2L/\mu$, the it holds that*

$$1075 \|\nabla \Phi(x) - \nabla \Phi_\lambda(x)\| \leq \mathcal{O}(\kappa^3/\lambda).$$

$$1076$$

$$1077$$

1078 Lemma 13 is a restatement of Lemma 3.1 by Kwon et al. (2023b), which demonstrates that when
1079 $\lambda \asymp \epsilon^{-1}$, an ϵ -first-order stationary point of $\Phi_\lambda(x)$ is also an $\mathcal{O}(\epsilon)$ -first-order stationary of $\Phi(x)$.
Then we can get the main conclusion for F²SA method.

1080

1081 **Theorem 5.** Suppose Assumptions 1-5 hold. Define $\Delta := \Phi(x_0) - \inf_{x \in \mathbb{R}^{d_x}} \Phi(x)$ and
 1082 supposed Δ are bounded. Set the parameters in Algorithm 3 as

$$1083 \quad \lambda \asymp \max \{3\kappa, L\kappa^3/\epsilon, L\kappa^2/\Delta\}, \quad \beta \asymp \mathcal{O}(\lambda^{-2}\kappa^{-2}), \quad \alpha = \frac{1}{(\lambda+1)L}, \quad (18)$$

1086 then it can find an ϵ -first-order stationary point of $\Phi(x)$ within $T = \mathcal{O}(\kappa^8\epsilon^{-2})$ iterations.
 1087

1088 **Proof.** Let L_Φ be the gradient Lipschitz constant of $\Phi(x)$. Let $\beta \leq 1/(2L_\Phi)$, then
 1089

$$1090 \quad \Phi(x_{t+1}) \leq \Phi(x_t) + \langle \nabla \Phi(x_t), x_{t+1} - x_t \rangle + \frac{L_\Phi}{2} \|x_{t+1} - x_t\|^2$$

$$1091 \quad \leq \Phi(x_t) - \left(\frac{\beta}{2} - \beta^2 L_\Phi \right) \|\nabla \Phi(x_t)\|^2 + \left(\frac{\beta}{2} + \beta^2 L_\Phi \right) \|\nabla \Phi(x_t) - \hat{\nabla} \Phi(x_t)\|^2.$$

1094 Firstly, we have $\|\nabla \Phi(x_t) - \hat{\nabla} \Phi(x_t)\| \leq \|\nabla \Phi(x_t) - \nabla \Phi_\lambda(x_t)\| + \|\nabla \Phi_\lambda(x_t) - \hat{\nabla} \Phi(x_t)\|$. Then,
 1095 according to Lemma 4.3 in Chen et al. (2024), we have $\|\nabla \Phi(x_t) - \nabla \Phi_\lambda(x_t)\| \leq \mathcal{O}(\epsilon)$.
 1096

1097 For $\|\nabla \Phi_\lambda(x_t) - \hat{\nabla} \Phi(x_t)\|$, according to their definitions, we have the following result.
 1098

$$1100 \quad \|\nabla \Phi_\lambda(x_t) - \hat{\nabla} \Phi(x_t)\|$$

$$1101 \quad \leq \|\nabla_x f(x_t, y_\lambda^*(x_t)) - \nabla_x f(x_t, \hat{y}_t)\|$$

$$1102 \quad + \lambda (\|\nabla_x g(x_t, y_\lambda^*(x_t)) - \nabla_x g(x_t, \hat{y}_t)\| + \|\nabla_x g(x_t, y^*(x_t)) - \nabla_x g(x_t, \hat{z}_t)\|)$$

$$1103 \quad \leq (\lambda+1)L \|y_\lambda^*(x_t) - \hat{y}_t\| + \lambda L \|y^*(x_t) - \hat{z}_t\|.$$

1105 For $\Delta y_t := \|y_\lambda^*(x_t) - \hat{y}_t\|$, according to Lemma B.3 in Kwon et al. (2023b), we have if $\lambda > 2L/\mu$,
 1106 then the function $h_\lambda(x, y)$ is $\lambda\mu/2$ -strong convex for y . Let $\alpha \leq \frac{1}{(\lambda+1)L}$, Then we have
 1107

$$1108 \quad \|y_\lambda^*(x_t) - \hat{y}_t\| \leq \left(1 - \alpha \frac{\lambda\mu}{2}\right) \|y_\lambda^*(x_t) - \hat{y}_t\|$$

$$1109 \quad \leq \left(1 - \alpha \frac{\lambda\mu}{2}\right) \|y_\lambda^*(x_{t-1}) - \hat{y}_{t-1}\| + \frac{3L}{\mu} \|x_t - x_{t-1}\|$$

$$1110 \quad \leq \left(1 - \alpha \frac{\lambda\mu}{2}\right) \|y_\lambda^*(x_{t-1}) - \hat{y}_{t-1}\| + \frac{3L\beta}{\mu} \|\hat{\nabla} \Phi(x_{t-1})\|.$$

1115 Similarly, for $\Delta z_t := \|y^*(x_t) - \hat{z}_t\|$, we have
 1116

$$1117 \quad \|y^*(x_t) - \hat{z}_t\| \leq (1 - \alpha\mu) \|y^*(x_{t-1}) - \hat{z}_{t-1}\| + \frac{3L\beta}{\mu} \|\hat{\nabla} \Phi(x_{t-1})\|.$$

1119 For $\|\hat{\nabla} \Phi(x_{t-1})\|$, we have
 1120

$$1122 \quad \|\hat{\nabla} \Phi(x_{t-1})\| \leq \|\hat{\nabla} \Phi(x_{t-1}) - \nabla \Phi_\lambda(x_{t-1})\| + \|\nabla \Phi_\lambda(x_{t-1}) - \nabla \Phi(x_{t-1})\| + \|\nabla \Phi(x_{t-1})\|$$

$$1123 \quad \leq (\lambda+1)L \|y_\lambda^*(x_{t-1}) - \hat{y}_{t-1}\| + \lambda L \|y^*(x_{t-1}) - \hat{z}_{t-1}\| + \mathcal{O}(\epsilon) + \|\nabla \Phi(x_{t-1})\|.$$

1125 Take the above results into $\Delta y_t + \Delta z_t$, then we have
 1126

$$1127 \quad \Delta y_t + \Delta z_t \leq \left(1 - \alpha \frac{\lambda\mu}{2}\right) \Delta y_{t-1} + \frac{3L\beta}{\mu} \|\hat{\nabla} \Phi(x_{t-1})\|$$

$$1128 \quad + (1 - \alpha\mu) \Delta z_{t-1} + \frac{3L\beta}{\mu} \|\hat{\nabla} \Phi(x_{t-1})\|$$

$$1129 \quad \leq (1 - \alpha\mu + \frac{3L\beta}{\mu}(\lambda+1)L) (\Delta y_{t-1} + \Delta z_{t-1}) + \frac{3L\beta}{\mu} (\mathcal{O}(\epsilon) + \|\nabla \Phi(x_{t-1})\|)$$

$$1130 \quad \leq D_2 (\Delta y_{t-1} + \Delta z_{t-1}) + D_1 + D_0 \|\nabla \Phi(x_{t-1})\|,$$

1134 where $D_0 = \frac{3L\beta}{\mu}$, $D_1 = \frac{3L\beta}{\mu} \mathcal{O}(\epsilon)$, $D_2 = 1 - \alpha\mu + \frac{3L\beta}{\mu}(\lambda + 1)L$. Let $D_2 \leq (1 - \alpha\mu/2)$, then we
 1135 have $\beta \leq \frac{\alpha\mu^2}{6(\lambda+1)L^2} \leq \frac{\mu^2}{6(\lambda+1)^2L^3}$. Combine the above results, we have
 1136

$$\begin{aligned} 1137 \Delta y_t + \Delta z_t &\leq D_2(\Delta y_{t-1} + \Delta z_{t-1}) + D_1 + D_0 \|\nabla \Phi(x_{t-1})\| \\ 1138 &\leq [D_2]^t (\Delta y_0 + \Delta z_0) + D_0 \sum_{i=0}^{t-1} [D_2]^{t-1-i} \|\nabla \Phi(x_i)\| + D_1 \frac{1 - [D_2]^t}{1 - D_2} \\ 1139 &\leq \left(1 - \frac{\alpha\mu}{2}\right)^t (\Delta y_0 + \Delta z_0) + D_0 \sum_{i=0}^{t-1} \left(1 - \frac{\alpha\mu}{2}\right)^{t-1-i} \|\nabla \Phi(x_i)\| + \frac{2D_1}{\alpha\mu}. \\ 1140 & \\ 1141 & \\ 1142 & \\ 1143 & \\ 1144 & \end{aligned}$$

1145 Thus, we have

$$1146 (\Delta y_t + \Delta z_t)^2 \leq 3 \left(1 - \frac{\alpha\mu}{4}\right)^t (\Delta y_0 + \Delta z_0)^2 + \frac{6[D_0]^2}{\alpha\mu} \sum_{i=0}^{t-1} \left(1 - \frac{\alpha\mu}{4}\right)^{t-1-i} \|\nabla \Phi(x_i)\|^2 + \frac{12[D_1]^2}{\alpha^2\mu^2}. \\ 1147 \\ 1148$$

1149 Thus, for $\|\nabla \Phi(x_t) - \hat{\nabla} \Phi(x_t)\|^2$, we have
 1150

$$\begin{aligned} 1151 \|\nabla \Phi(x_t) - \hat{\nabla} \Phi(x_t)\|^2 & \\ 1152 &\leq 2 \|\nabla \Phi(x_t) - \nabla \Phi_\lambda(x_t)\|^2 + 2 \|\nabla \Phi_\lambda(x_t) - \hat{\nabla} \Phi(x_t)\|^2 \\ 1153 &\leq 2\mathcal{O}(\epsilon^2) + 2(\lambda + 1)^2 L^2 (\Delta y_t + \Delta z_t)^2 \\ 1154 &\leq 2\mathcal{O}(\epsilon^2) + 6(\lambda + 1)^2 L^2 \left(1 - \frac{\alpha\mu}{4}\right)^t (\Delta y_0 + \Delta z_0)^2 + \frac{12(\lambda + 1)^2 L^2 [D_0]^2}{\alpha\mu} \sum_{i=0}^{t-1} \left(1 - \frac{\alpha\mu}{4}\right)^{t-1-i} \|\nabla \Phi(x_i)\|^2 \\ 1155 & \\ 1156 &\quad + \frac{24(\lambda + 1)^2 L^2 [D_1]^2}{\alpha^2\mu^2} \\ 1157 & \\ 1158 & \\ 1159 & \\ 1160 & \\ 1161 & \\ 1162 & \\ 1163 & \\ 1164 & \\ 1165 & \\ 1166 & \\ 1167 & \end{aligned}$$

1166 where $D_3 = 6(\lambda + 1)^2 L^2 (\Delta y_0 + \Delta z_0)^2$, $D_4 = \frac{12(\lambda + 1)^2 L^2 [D_0]^2}{\alpha\mu}$, $D_5 = \frac{24(\lambda + 1)^2 L^2 [D_1]^2}{\alpha^2\mu^2} + 2\mathcal{O}(\epsilon^2)$.
 1167 Then we have

$$\begin{aligned} 1168 \Phi(x_{t+1}) &\leq \Phi(x_t) - \left(\frac{\beta}{2} - \beta^2 L_\Phi\right) \|\nabla \Phi(x_t)\|^2 \\ 1169 &+ \left(\frac{\beta}{2} + \beta^2 L_\Phi\right) \left(D_3 \left(1 - \frac{\alpha\mu}{4}\right)^t + D_4 \sum_{i=0}^{t-1} \left(1 - \frac{\alpha\mu}{4}\right)^{t-1-i} \|\nabla \Phi(x_i)\|^2 + D_5\right). \\ 1170 & \\ 1171 & \\ 1172 & \\ 1173 & \end{aligned}$$

1174 Telescoping the above equation over t from 0 to $T - 1$ yields

$$\begin{aligned} 1175 \Phi(x_T) &\leq \Phi(x_0) - \left(\frac{\beta}{2} - \beta^2 L_\Phi\right) \sum_{t=0}^{T-1} \|\nabla \Phi(x_t)\|^2 + \left(\frac{\beta}{2} + \beta^2 L_\Phi\right) \left(\frac{4D_4}{\alpha\mu} \sum_{t=0}^{T-1} \|\nabla \Phi(x_t)\|^2\right) \\ 1176 &+ \left(\frac{\beta}{2} + \beta^2 L_\Phi\right) \frac{4D_3}{\alpha\mu} + \left(\frac{\beta}{2} + \beta^2 L_\Phi\right) D_5 T. \\ 1177 & \\ 1178 & \\ 1179 & \\ 1180 & \end{aligned}$$

1181 Let $A = \frac{\beta}{2} - \beta^2 L_\Phi - \frac{4D_4}{\alpha\mu} \left(\frac{\beta}{2} + \beta^2 L_\Phi\right)$, $B = \left(\frac{\beta}{2} + \beta^2 L_\Phi\right) D_5$, then we have
 1182

$$1183 \frac{1}{T} \sum_{t=0}^{T-1} \|\nabla \Phi(x_t)\|^2 \leq \frac{\Phi(x_0) - \inf \Phi(x) + \frac{4D_3}{\alpha\mu} \left(\frac{\beta}{2} + \beta^2 L_\Phi\right)}{AT} + \frac{B}{A}. \\ 1184 \\ 1185$$

1186 Since we can choose the initial y_0 in a BOX to let $(\Delta y_0 + \Delta z_0)^2 \leq \mathcal{O}(\kappa)$, we focus on the order of
 1187 A and B . Firstly, let $\beta \leq \min\{\frac{\mu^2}{12(\lambda+1)^2 L^3}, \frac{1}{4L_\Phi}\}$ to make $A > 0$. Because $\lambda > 2L/\mu = \mathcal{O}(\kappa)$, we

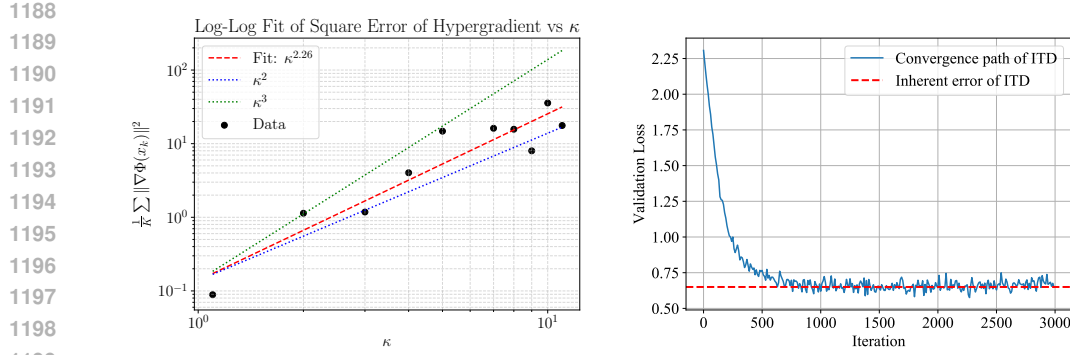


Figure 3: **Left:** Comparison of error curves of the single-loop ITD-based Algorithm on the task of feature learning (Bao et al., 2021) of the space dataset (Chang & Lin, 2011). Curves of the upper bound of $\frac{1}{K} \sum \|\Phi(x_k)\|^2$ with respect to different condition numbers κ . **Right:** Verification of the inherent error of the single-loop ITD-based Algorithm. We conduct data reweighting experiment on the MNIST dataset LeCun et al. (1998) with 20% label corruption. The validation loss ultimately exhibits an inherent error of approximately 0.65.

have $\beta = \mathcal{O}(\lambda^{-2}\kappa^{-2}) \leq \mathcal{O}(\kappa^{-4})$. Then, for B , let $D_5 = \mathcal{O}(\epsilon^2)$, then we have $\beta \asymp \frac{\alpha\mu}{6\sqrt{6}(\lambda+1)L^2} \asymp \mathcal{O}(\lambda^{-2}\kappa^{-2})$. On the other hand, because we must control the gap between $\nabla\Phi(x)$ and $\nabla\Phi_\sigma(x)$, according to Lemma 13, we let $\lambda \asymp \mathcal{O}(\kappa^3\epsilon^{-1})$. Thus, we have $\beta \asymp \mathcal{O}(\kappa^{-8})$ to let all the conditions satisfied. Finally, combined the parameters in Eq. (18), then to achieve ϵ -first-order stationary point, we need $T = \mathcal{O}(\kappa^8\epsilon^{-2})$. \square

Remark 7. Kwon et al. (2023b) established an $\mathcal{O}(\epsilon^{-3})$ convergence rate for the F^2 SA algorithm to ϵ -first-order stationary point but did not characterize its dependence on κ . In comparison, we improve the convergence rate with respect to $\mathcal{O}(\kappa^8\epsilon^{-2})$. To the best of our knowledge, this is the first result achieving an $\mathcal{O}(\epsilon^{-2})$ convergence rate for a single-loop F^2 SA algorithm. This improvement is enabled by the analytical tools we introduce and our refined analysis.

Our theoretical findings are consistent with the assertion by Kwon et al. (2023b) that, when the stepsize of outer-level is sufficiently small, the F^2 SA algorithm effectively reduces to a single-loop scheme. Moreover, we provide a non-asymptotic condition on the stepsize, requiring it to satisfy $\mathcal{O}(\lambda^{-2}\kappa^2)$.

D ADDITIONAL EXPERIMENTS

D.1 EXPERIMENTAL SETTINGS

In our experiments, we consider two widely used tasks, feature learning (Franceschi et al., 2018) and data reweighting for noisy labels (Shaban et al., 2019).

For feature learning (Franceschi et al., 2018; Bao et al., 2021), we evaluate the regression problem on the space dataset (Chang & Lin, 2011). We randomly select 500 and 500 images for training and validation respectively. The outer variable x represents the parameters in a linear layer of size $6 \rightarrow 128$ to extract features. The inner variable y represents the parameters in a linear layer of size $128 \rightarrow 1$ to predict the value. The total iteration size is 10000.

For data reweighting, we evaluate a classification problem on the MNIST dataset following Shaban et al. (2019); Bao et al. (2021). MNIST consists of grayscale handwritten digits of size 28×28 . We randomly select 2000 and 500 images for training and validation respectively. The label of a training sample is replaced by a uniformly sampled wrong label with probability 0.2. x represents the logits of the weights of the training data, and y represents the parameters in an MLP of size $784 \rightarrow 256 \rightarrow 10$. The learning rate is $1e^{-3}$ in the outer-level and $5e^{-2}$ in the inner-level. The total iteration size is 3000.

1242
1243

D.2 RESULTS

1244
1245
1246
1247
1248
1249
1250
1251
1252

Results of feature learning. To evaluate the effectiveness of our theoretical findings, we carry out experiments focusing on the ITD-based algorithm with the mentioned feature learning task. By modifying the singular values of the feature matrix in the training set, we were able to directly control the condition number κ . The final experimental results are shown in Figure 3 (**Left**). For different values of the condition number κ , we record the mean squared norm of the hypergradient $\frac{1}{K} \sum_{k=0}^{K-1} \|\Phi(x_k)\|^2$ (which can be computed exactly using the closed-form solution of the head layer). The results demonstrate that the empirical dependence between the hypergradient's mean squared norm and the condition number follows $\mathcal{O}(\kappa^{2.26})$. This dependence is closer to $\mathcal{O}(\kappa^2)$ than to $\mathcal{O}(\kappa^3)$, thereby supporting the soundness of our theoretical conclusions.

1253
1254
1255

Moreover, the observed exponent $\mathcal{O}(\kappa^{2.26})$ is likely due to limitations on the number of iterations, which prevent the term $\mathcal{O}(\kappa^3/K)$ from becoming negligible. As a result, the final empirical rate appears as $\mathcal{O}(\kappa^{2.26})$, lying closer to $\mathcal{O}(\kappa^2)$, consistent with our theoretical predictions.

1256
1257
1258
1259
1260
1261

Results of data reweighting. Figure 3 (**Right**) illustrates the convergence path of the validation loss for single-loop ITD-based algorithms in the data-reweighting task. As the number of iterations increases, the outer-level validation loss decreases rapidly and then stays near a fixed value (approximately 0.65 in this experiment). This observation indicates that single-loop ITD methods indeed exhibit an inherent, non-vanishing error, which supports the soundness of our theoretical results.

1262
1263

E EXTENSION TO OTHER PROBLEMS

1264
1265
1266

In this section, we will show that our technique is possible to analyze the bilevel optimization algorithms and the other problem settings, such as the multi-loop, the stochastic bilevel problem, and minimax problem.

1267
1268
1269
1270
1271

Multi-loop bilevel problem. The analysis of both existing single-loop and multi-loop methods for bilevel optimization are based on providing the upper bound of $\|\nabla\Phi(x_k) - \widehat{\nabla}\Phi(x_k)\|^2$, $\Delta v_k := \|v_k^* - \hat{v}_k\|$, and $\Delta y_k := \|y_k^* - \hat{y}_k\|$. For example, The proof of Ji et al. (2022) is based on establishing the inequalities:

1272
1273
1274
1275

$$\begin{aligned} \|\nabla\Phi(x_k) - \widehat{\nabla}\Phi(x_k)\|^2 &\leq C_1[\Delta y_k]^2 + C_2[\Delta v_k]^2; \\ [\Delta v_k]^2 &\leq C_{v,1}(Q)[\Delta v_{k-1}]^2 + C_{v,2}(N)[\Delta y_{k-1}]^2 + C_{v,3}\|\nabla\Phi(x_{k-1})\|^2; \\ [\Delta y_k]^2 &\leq C_{y,1}(N)[\Delta y_{k-1}]^2 + C_{y,2}[\Delta v_{k-1}]^2 + C_{y,3}\|\nabla\Phi(x_{k-1})\|^2. \end{aligned}$$

1276
1277
1278
1279

where C_1 , C_2 , $C_{v,3}$, $C_{y,2}$, and $C_{y,3}$ are positive constants, $C_{v,1}(\cdot)$, $C_{v,2}(\cdot)$, $C_{v,3}(\cdot)$, $C_{y,1}(\cdot)$, and $C_{y,3}(\cdot)$ are positive constants related to the iteration steps, and Q , N , and k denote the iteration steps of the variables v , y , and x , respectively.

1280

Our key analysis is different from the above framework. Specifically, we establish the inequalities

1281
1282
1283

$$\begin{aligned} \|\nabla\Phi(x_k) - \widehat{\nabla}\Phi(x_k)\|^2 &\leq [C'_1(\Delta y_k + C'_2(Q, N)\Delta v_k)]^2; \\ \Delta y_k + C'_2(Q, N)\Delta v_k &\leq C'_3(\Delta y_{k-1} + C'_2(Q, N)\Delta v_{k-1} + C'_4\|\nabla\Phi(x_{k-1})\|), \end{aligned}$$

1284
1285
1286
1287

where C'_1 , C'_3 , and C'_4 are positive constants, $C'_2(\cdot, \cdot)$ is a positive constant related to Q and N . Since the above results also provide the upper bound for $\|\nabla\Phi(x_k) - \widehat{\nabla}\Phi(x_k)\|^2$, Δv_k , and Δy_k , our framework can work both for single-loop and multi-loop methods.

1288
1289
1290
1291
1292
1293
1294
1295

Stochastic bilevel problem. For the stochastic analysis, the key steps in our analysis for the deterministic setting $\Delta y_k \leq C_1\Delta y_{k-1} + C_2\|\nabla\Phi(x_{k-1})\|$ and $\|\nabla\Phi(x_k) - \widehat{\nabla}\Phi(x_k)\| \leq C_3\Delta y_k + C_4\|\hat{v}_k - \tilde{v}_k\|$ can be extended to $\mathbb{E}[\Delta y_k] \leq C_1\mathbb{E}[\Delta y_{k-1}] + C_2\|\nabla\Phi(x_{k-1})\| + C_\sigma$ and $\|\nabla\Phi(x_k) - \widehat{\nabla}\Phi(x_k)\| \leq C_3\Delta y_k + C_4\|\mathbb{E}[\hat{v}_k] - \mathbb{E}[\tilde{v}_k]\| + C_5\|\hat{v}_k\| + C_6$, where C_1 - C_6 are positive constants, C_σ is a positive constant related to the variance of ∇g . By setting the learning rates of $\alpha = \frac{1}{L}$ and $\beta = \mathcal{O}(\kappa^{3.5}k^{-0.5})$, we can control the right-hand side of above inequalities, then achieve the result for stochastic setting by following the other parts of our framework.

Minimax problem. We can also apply our technique to solve the nonconvex-strongly-concave minimax problem $\min_x \max_y f(x, y)$. Specifically, we can set $g = -f$ for our framework, which

1296 leads to the hypergradient $\nabla f(x, y^*(x)) = -\nabla_x g(x, y^*(x))$ and achieves results for finding the
1297 stationary point of $\nabla\Phi(x)$ accordingly.
1298

1299 **F THE USE OF LARGE LANGUAGE MODELS**
1300

1301 In preparing this paper, we made limited use of ChatGPT (an OpenAI large language model) solely
1302 for language polishing and minor improvements in clarity and readability of a few sections. The
1303 LLM did not contribute to research ideation, technical content, experimental design, analysis, or
1304 writing of substantive material. All research ideas, methods, results, and conclusions are entirely
1305 those of the authors.
1306

1307
1308
1309
1310
1311
1312
1313
1314
1315
1316
1317
1318
1319
1320
1321
1322
1323
1324
1325
1326
1327
1328
1329
1330
1331
1332
1333
1334
1335
1336
1337
1338
1339
1340
1341
1342
1343
1344
1345
1346
1347
1348
1349